

Bayesian Function-on-Scalars Regression for High Dimensional Data

Daniel R. Kowal and Daniel C. Bourgeois ^{*†}

March 16, 2022

Abstract

We develop a fully Bayesian framework for function-on-scalars regression with many predictors. The functional data response is modeled nonparametrically using unknown basis functions, which produces a flexible and data-adaptive functional basis. We incorporate shrinkage priors that effectively remove unimportant scalar covariates from the model and reduce sensitivity to number of (unknown) basis functions. For variable selection in functional regression, we propose a *decoupled shrinkage and selection* technique, which identifies a small subset of covariates that retains nearly the predictive accuracy of the full model. Our novel approach is broadly applicable for Bayesian functional regression models, and unlike existing methods provides joint rather than marginal selection of important predictor variables. Computationally scalable posterior inference is achieved using a Gibbs sampler with linear time complexity in the number of predictors. The resulting algorithm is empirically faster than existing frequentist and Bayesian techniques, and provides joint estimation of model parameters, prediction and imputation of functional trajectories, and uncertainty quantification via the posterior distribution. A simulation study demonstrates substantial improvements in estimation accuracy, uncertainty quantification, and variable selection relative to existing alternatives. The methodology is applied to actigraphy data to investigate the association between intraday physical activity and responses to a sleep questionnaire.

KEYWORDS: shrinkage; factor model; variable selection; actigraphy data; MCMC

^{*}Kowal is Assistant Professor, Department of Statistics, Rice University, Houston, TX 77251-1892 (E-mail: Daniel.Kowal@rice.edu). Bourgeois is a PhD student, Department of Statistics, Rice University, Houston, TX 77251-1892 (E-mail: Daniel.C.Bourgeois@rice.edu)

[†]This material is based upon work supported by the National Science Foundation Graduate Research Fellowship (Bourgeois) under Grant DGE-1450681 and partially supported by NSF award #1547433 RTG: Cross-training in Statistics and Computer Science.

1 Introduction

Modern scientific measuring systems commonly record data over a continuous domain, often at high resolutions, and referred to as *functional data*. Functional data are typically high dimensional and highly correlated, and may be measured concurrently with other variables of interest. We consider the problem of *function-on-scalars regression* (FOSR), in which a functional data response is modeled using (possibly many) *scalar* predictors. Applications of FOSR are broad and impactful: examples include blood pressure profiles during pregnancy (Montagna et al., 2012), human motor control following a stroke (Chen et al., 2016), age-specific fertility rates (Kowal, 2018), microarray time course gene expression data (Wang et al., 2007), and longitudinal genome-wide association studies (Barber et al., 2017; Fan and Reimherr, 2017), among others (Ramsay and Silverman, 2005; Morris, 2015).

FOSR shares the same fundamental goals as multiple regression: estimation and inference for the regression coefficients, variable selection of important predictor variables, and prediction of new responses. However, the functional data response in FOSR introduces additional modeling challenges. Within-curve dependence of functional data requires careful modeling of the covariance function, which may be complex, with implications for computational scalability. In addition, the regression coefficients in FOSR are *functions*, which substantially complicates estimation, inference, and selection. Naturally, these challenges are compounded in higher-dimensional settings with many predictors. Lastly, prediction in FOSR requires prediction of functional trajectories, which may be partially observed.

To address these challenges, we develop a fully Bayesian framework for FOSR, where the number of predictors p may be greater than the number of observed curves n . Within-curve dependence is modeled nonparametrically using *unknown* basis functions, which produces a data-adaptive functional basis with uncertainty quantification via the posterior distribution. We introduce shrinkage priors for functional regression that mitigate the impact of unimportant predictor variables and reduce sensitivity to the dimension of the (unknown)

functional basis. A simulation study confirms the importance of these shrinkage priors and demonstrates clear improvements in statistical efficiency relative to existing FOSR models. For computationally scalable posterior inference, we develop a Gibbs sampling algorithm with linear time complexity in either n or p . The methodology is applicable for densely- or sparsely-observed functional data, with automatic prediction and imputation at unobserved points within the Gibbs sampler.

Recent developments in FOSR have focused on variable selection, particularly in the frequentist literature. Variable selection in FOSR requires selecting or thresholding entire regression coefficient *functions*. Accordingly, various group penalties have been proposed for variable selection in FOSR, including a group smoothly clipped absolute deviation (SCAD; Wang et al., 2007) and a group-minimax concave penalty (MCP; Chen et al., 2016) for a moderate number of predictors, and a group lasso (Barber et al., 2017) and an adaptive group lasso (Fan and Reimherr, 2017) for high-dimensional predictors. Although these frequentist methods provide both estimation and selection, finite-sample inference is unavailable and important tuning parameters must be selected, which is often computationally intensive. By comparison, Bayesian approaches provide exact finite-sample inference (usually up to MCMC error) and do not require selection of tuning parameters. Bayesian FOSR models may include shrinkage priors (Zhu et al., 2011; Kowal, 2018) and identify important predictors marginally using *global Bayesian p-values* (GBPVs); see Meyer et al. (2015). However, there is currently no coherent Bayesian framework for simultaneous estimation, inference, and variable selection in FOSR, particularly for a moderate to large number of predictors.

We provide Bayesian variable selection for FOSR by extending the *decoupling shrinkage and selection* (DSS) approach of Hahn and Carvalho (2015) to the functional data setting. DSS offers a framework for selecting a small subset of predictors that maintains nearly the predictive accuracy of the full model, as determined by the posterior distribution. The tradeoff between predictive accuracy and sparsity is determined by a loss function, which is applicable for a variety of models and priors. Despite its generality, DSS has not yet been

developed for functional regression. Our novel DSS approach performs variable selection on regression coefficients *functions*, and is broadly applicable for Bayesian functional regression models. The proposed method selects predictor variables *jointly*, and improves upon the frequentist group lasso and (marginal) Bayesian variable selection using GBPVs.

We apply our methods to study the association between intraday physical activity and responses to a sleep questionnaire among elderly adults. The dataset, obtained from the National Sleep Research Resource (Dean et al., 2016; Zhang et al., 2018), consists of actigraphy data measuring activity as a function of time-of-day, demographic variables (age, gender, and race/ethnicity), and responses to a sleep questionnaire summarized in Table 2. It is *a priori* unclear which questionnaire items, if any, are associated with physical activity, and whether or not such associations vary throughout the day. The proposed methodology provides the framework to (i) model and impute complex intraday physical activity trajectories for each individual, (ii) estimate regression coefficient functions and accompanying posterior credible bands, and (iii) select a small subset of the $p = 74$ demographic variables and questionnaire items that maintain nearly the predictive accuracy of the full model.

The remainder of the paper is organized as follows: the model is in Section 2; computational results are in Section 3; the variable selection method is in Section 4; a simulation analysis is in Section 5; the application is in Section 6; we conclude in Section 7. The MCMC algorithm, theoretical results, and details on the sleep questionnaire are in the Appendix. MCMC diagnostics and details on the application are provided in the supplement.

2 A Bayesian Function-on-Scalars Regression Model

2.1 Model Specification and Assumptions

Let Y_1, \dots, Y_n be a sample of random functions in $L^2(\mathcal{T})$, where $\mathcal{T} \subset \mathbb{R}^D$ is a compact index set and $D \in \mathbb{Z}^+$. Suppose we have p scalar predictors $\{x_{i,j}\}_{j=1}^p$ for $i = 1, \dots, n$, possibly with $p > n$. We are interested in modeling the association between the scalar predictors $x_{i,j}$ and

the functional response Y_i . We propose the following Bayesian function-on-scalars regression (FOSR) model:

$$Y_i(\tau) = \sum_{k=1}^K f_k(\tau)\beta_{k,i} + \epsilon_i(\tau), \quad \epsilon_i(\tau) \stackrel{indep}{\sim} N(0, \sigma_\epsilon^2), \quad \tau \in \mathcal{T} \quad (1)$$

$$\beta_{k,i} = \mu_k + \sum_{j=1}^p x_{i,j}\alpha_{j,k} + \gamma_{k,i} \quad (2)$$

$$\mu_k \stackrel{indep}{\sim} N(0, \sigma_{\mu_k}^2), \quad \alpha_{j,k} \stackrel{indep}{\sim} N(0, \sigma_{\alpha_{j,k}}^2), \quad \gamma_{k,i} \stackrel{indep}{\sim} N(0, \sigma_{\gamma_{k,i}}^2) \quad (3)$$

Model (1)-(3) is completed by specifying prior distributions on the variance components σ_ϵ^2 , $\sigma_{\mu_k}^2$, $\sigma_{\alpha_{j,k}}^2$, and $\sigma_{\gamma_{k,i}}^2$ (Section 2.2) and the functions $\{f_k(\cdot)\}$ (Section 2.3). We assume a Jeffreys' prior for the observation error variance, $[\sigma_\epsilon^2] \propto 1/\sigma_\epsilon^2$. Note that the distributions in (1) and (3) are *conditionally* Gaussian, so careful choice of priors for the accompanying variance components will produce a variety of marginal distributions (Wand et al., 2011).

Model (1) decomposes the functional data $Y_i(\tau)$ into a linear combination of K *loading curves*, $\{f_k(\tau)\}_{k=1}^K$, and *factors*, $\{\beta_{k,i}\}_{k=1}^K$. The loading curves capture within-curve dependence of the functional data Y_i , while the factors model between-curve dependence induced by the predictor variables $x_{i,j}$. Each f_k is modeled nonparametrically using *low-rank thin plate splines*, which are well-defined for $\mathcal{T} \subset \mathbb{R}^D$ with $D \in \mathbb{Z}^+$ and are smooth, flexible, and efficient for computations (Ruppert et al., 2003; Wood, 2006). The $\{f_k\}$ may be interpreted as a common yet unknown functional basis for Y_i with unknown basis coefficients $\{\beta_{k,i}\}$. By modeling the $\{f_k\}$ as unknown, and imposing suitable identifiability constraints (see Section 2.3), our model incorporates the uncertainty of $\{f_k\}$ into the posterior distribution for all parameters of interest, which is necessary for valid inference.

In (2)-(3), we introduce a regression model for the factors $\{\beta_{k,i}\}$ with conditionally Gaussian priors for the intercepts $\{\mu_k\}$, the regression coefficients $\{\alpha_{j,k}\}$, and the subject-specific errors $\{\gamma_{k,i}\}$. Each term is k -specific, and therefore its association with $Y_i(\tau)$ may be interpreted via $f_k(\tau)$. The priors in (3) are selected to achieve desired shrinkage effects, and are

important in functional regression with many predictors; see Section 2.2 for details.

Model (1)-(3) may be expressed as a more conventional FOSR model. Let $\mathcal{GP}(c, C)$ denote a Gaussian process with mean function c and covariance function C .

Proposition 1. *Model (1)-(3) implies the functional regression model*

$$Y_i(\tau) = \tilde{\mu}(\tau) + \sum_{j=1}^p x_{i,j} \tilde{\alpha}_j(\tau) + \tilde{\gamma}_i(\tau) + \epsilon_i(\tau), \quad \epsilon_i(\tau) \stackrel{\text{indep}}{\sim} N(0, \sigma_\epsilon^2), \quad \tau \in \mathcal{T} \quad (4)$$

$$\tilde{\mu}(\cdot) \stackrel{\text{indep}}{\sim} \mathcal{GP}(0, C_\mu), \quad \tilde{\alpha}_j(\cdot) \stackrel{\text{indep}}{\sim} \mathcal{GP}(0, C_{\alpha_j}), \quad \tilde{\gamma}_i(\cdot) \stackrel{\text{indep}}{\sim} \mathcal{GP}(0, C_{\gamma_i}) \quad (5)$$

with expansions $\tilde{\mu}(\tau) = \sum_{k=1}^K f_k(\tau) \mu_k$, $\tilde{\alpha}_j(\tau) = \sum_{k=1}^K f_k(\tau) \alpha_{j,k}$, $\tilde{\gamma}_i(\tau) = \sum_{k=1}^K f_k(\tau) \gamma_{k,i}$ and covariance functions $C_\mu(\tau, u) = \sum_{k=1}^K f_k(\tau) f_k(u) \sigma_{\mu_k}^2$, $C_{\alpha_j}(\tau, u) = \sum_{k=1}^K f_k(\tau) f_k(u) \sigma_{\alpha_{j,k}}^2$, and $C_{\gamma_i}(\tau, u) = \sum_{k=1}^K f_k(\tau) f_k(u) \sigma_{\gamma_{k,i}}^2$.

The predictors $x_{i,j}$ are directly associated with the functional data $Y_i(\tau)$ via the regression coefficient functions $\tilde{\alpha}_j(\tau) = \sum_k f_k(\tau) \alpha_{j,k}$. Since the MCMC algorithm (see Appendix) produces posterior draws of $\{f_k\}$ and $\{\alpha_{j,k}\}$, posterior inference for $\tilde{\alpha}_j(\tau)$ is readily available. The subject-specific error term $\tilde{\gamma}_i(\tau)$ in (4) captures within-curve variability in $Y_i(\tau)$ unexplained by $\{x_{i,j}\}$, which marginally produces a model for within-curve correlations of the FOSR error. Accounting for within-curve error correlations is important for statistically efficient estimation and valid inference in FOSR (Reiss et al., 2010), especially for high-dimensional predictors (Chen et al., 2016).

Existing approaches for FOSR commonly estimate model (4) using basis expansions. The dimension of the basis is important: a K -dimensional basis requires estimation of K coefficients for each predictor variable $j = 1, \dots, p$. Full basis expansions, such as splines or wavelets, have been successfully applied for a small to moderate number of predictors (Ramsay and Silverman, 2005), with extensions for functionally correlated errors (Reiss et al., 2010) and mixed effects models (Brumback and Rice, 1998; Guo, 2002; Morris and Carroll, 2006; Zhu et al., 2011; Goldsmith and Kitago, 2016). However, for a moderate to large

number of predictors, FOSR models using full basis expansions are neither parsimonious nor computationally scalable. As a remedy, an alternative approach is to pre-compute a lower-dimensional basis, such as a functional principal components (FPC) basis (e.g., Shang, 2014). While this approach reduces the number of parameters and improves computational scalability, it implicitly conditions on the estimated basis functions and therefore ignores the inherent uncertainty. Goldsmith et al. (2013) find that FPC-based methods can substantially underestimate total variability, even for densely-sampled functional data.

Bayesian reduced-rank models provide a natural framework for incorporating the uncertainty in the unknown $\{f_k\}$. Suarez et al. (2017) propose a Bayesian FPC model without predictors. Montagna et al. (2012) include predictors in a functional factor model, but do not use shrinkage priors to reduce the impact of unimportant variables, which is essential for moderate to large p . In addition, Montagna et al. (2012) model the unknown basis functions using Gaussian processes with known hyperparameters, which is restrictive and scales poorly in the number of observation points m . Goldsmith et al. (2015) propose a multilevel reduced-rank model for exponential family distributions using a Hamiltonian Monte Carlo algorithm for estimation and inference; however, the algorithm is not scalable in n , p , or m . Kowal et al. (2017a) and Kowal (2018) introduce reduced-rank functional data models for time-ordered functional data with dynamic predictors, but do not exploit vital computational simplifications developed for FOSR in Section 3 and as a result scale poorly in p .

2.2 Shrinkage Priors

Shrinkage priors are an important component of model (1)-(3). The regression model (2) may include unimportant predictors, especially for moderate to large p . Without regularization or shrinkage, such irrelevant predictors can reduce estimation accuracy and statistical efficiency. Model (1)-(3) also requires a choice of K , which determines the rank of the cross-covariance function. While K may be treated as unknown and estimated in the model, this approach typically requires computationally intensive procedures, such as reversible

jump MCMC (Suarez et al., 2017). Instead, we impose ordered shrinkage with respect to $k = 1, \dots, K$, so that larger number factors are *a priori* less important. Ordered shrinkage is computationally scalable and empirically reduces sensitivity to the choice of K , provided K is chosen sufficiently large.

We include a groupwise horseshoe prior for the regression coefficients $\alpha_{j,k} \stackrel{indep}{\sim} N(0, \sigma_{\alpha_{j,k}}^2)$, which extends Carvalho et al. (2010). Shrinkage is applied at both the factor-within-predictor level as well as the predictor-level using a hierarchy of half-Cauchy distributions:

$$\sigma_{\alpha_{j,k}} \stackrel{iid}{\sim} C^+(0, \lambda_j), \quad \lambda_j \stackrel{iid}{\sim} C^+(0, \lambda_0), \quad \lambda_0 \stackrel{iid}{\sim} C^+(0, p^{-1/2}) \quad (6)$$

for $j = 1, \dots, p$ and $k = 1, \dots, K$. The scale parameter $\sigma_{\alpha_{j,k}}$ controls the factor k shrinkage for predictor j , λ_j determines the shrinkage for all regression coefficients $\{\alpha_{j,k}\}_{k=1}^K$ for predictor j , and λ_0 corresponds to the global level of sparsity for all predictors $j = 1, \dots, p$, and is scaled by $p^{-1/2}$ following Piironen and Vehtari (2016). The horseshoe prior and its variants have been successful in a variety of models and applications, including functional regression (Kowal et al., 2017b; Kowal, 2018).

For ordered shrinkage, we apply the multiplicative gamma process (MGP) of Bhattacharya and Dunson (2011). MGP priors for the intercepts $\{\mu_k\}$ and the subject-specific errors $\{\gamma_{k,i}\}$ are represented via priors on the respective variance components in (3). The intercept prior precisions are $\sigma_{\mu_k}^{-2} = \prod_{\ell \leq k} \delta_{\mu_\ell}$, where $\delta_{\mu_1} \sim \text{Gamma}(a_{\mu_1}, 1)$ and $\delta_{\mu_\ell} \sim \text{Gamma}(a_{\mu_2}, 1)$ for $\ell > 1$, which implies a stochastic ordering for $\sigma_{\mu_k}^2$ when $a_{\mu_1} > 0$ and $a_{\mu_2} \geq 2$ (Bhattacharya and Dunson, 2011). For the subject-specific errors, we let $\sigma_{\gamma_{k,i}}^2 = \sigma_{\gamma_k}^2 / \xi_{\gamma_{k,i}}$ with $\sigma_{\gamma_k}^{-2} = \prod_{\ell \leq k} \delta_{\gamma_\ell}$, $\delta_{\gamma_1} \sim \text{Gamma}(a_{\gamma_1}, 1)$, $\delta_{\gamma_\ell} \sim \text{Gamma}(a_{\gamma_2}, 1)$ for $\ell > 1$, and $\xi_{\gamma_{k,i}} \stackrel{iid}{\sim} \text{Gamma}(\nu_\gamma/2, \nu_\gamma/2)$, as in Bhattacharya and Dunson (2011) and Montagna et al. (2012). We allow the data to determine the rate of ordered shrinkage separately for $\{\mu_k\}$ and $\{\gamma_{k,i}\}$ using the hyperpriors $a_{\mu_1}, a_{\mu_2}, a_{\gamma_1}, a_{\gamma_2} \stackrel{iid}{\sim} \text{Gamma}(2, 1)$. Lastly, the hyperprior $\nu_\gamma \sim \text{Uniform}(2, 128)$ induces heavy tails in the marginal distribution of $\gamma_{k,i}$ for additional model robustness.

2.3 Modeling the Loading Curves

We model each loading curve f_k as a smooth, unknown function and impose suitable identifiability constraints. Smoothness encourages information sharing among nearby points, which reduces variability to produce more stable prediction and imputation at unobserved points. Identifiability provides interpretability of the k -specific terms in model (1)-(3), in particular the regression coefficients $\alpha_{j,k}$. A key feature of our approach is that we construct identifiability constraints that are both computationally convenient to enforce on $\{f_k\}$ and provide massive computational simplifications for sampling model parameters in (2)-(3). Our model for $\{f_k\}$ closely follows Kowal (2018), so we omit details for brevity.

Suppose we observe the functional data Y_i at observation points $\{\tau_\ell\}_{\ell=1}^m$. For notational convenience, we assume the observation points are identical for all subjects i , but later relax that assumption in the case of sparsely- or irregularly-sampled functional data (see Section 6). For observed data $\mathbf{Y}_i = (Y_i(\tau_1), \dots, Y_i(\tau_m))'$, the likelihood in (1) becomes

$$\mathbf{Y}_i = \sum_{k=1}^K \mathbf{f}_k \beta_{k,i} + \boldsymbol{\epsilon}_i, \quad \boldsymbol{\epsilon}_i \sim N(\mathbf{0}, \sigma_\epsilon^2 \mathbf{I}_m) \quad (7)$$

where $\mathbf{f}_k = (f_k(\tau_1), \dots, f_k(\tau_m))'$ are the loading curves evaluated at the observation points.

We assume the basis expansions $f_k(\tau) = \mathbf{b}'(\tau)\boldsymbol{\psi}_k$, where $\mathbf{b}'(\tau) = (b_1(\tau), \dots, b_{L_m}(\tau))$ is an L_m -dimensional vector of *known* basis functions and $\boldsymbol{\psi}_k$ is an L_m -dimensional vector of *unknown* basis coefficients. We use *low rank thin plate splines* (LR-TPS), which are well-defined for $\mathcal{T} \subset \mathbb{R}^D$ with $D \in \mathbb{Z}^+$, smooth, flexible, and efficient in MCMC samplers (Crainiceanu et al., 2005). LR-TPS require selecting the number and location of knots. However, when paired with a roughness penalty on f_k , Ruppert (2002) note that LR-TPS estimates are not sensitive to the number and location of knots, provided there are enough knots in densely-observed regions of \mathcal{T} . We select knots following Ruppert et al. (2003) and Kowal (2018) and incorporate a roughness penalty via the prior $\boldsymbol{\psi}_k \sim N(\mathbf{0}, \lambda_{f_k}^{-1} \boldsymbol{\Omega}^{-1})$, where $\boldsymbol{\Omega}$ is a $L_m \times L_m$ known roughness penalty matrix. The smoothing parameter $\lambda_{f_k} > 0$

appears as a prior precision, so we assign a uniform prior distribution on the corresponding standard deviation, $\lambda_{f_k}^{-1/2} \stackrel{iid}{\sim} \text{Uniform}(0, 10^4)$ (Gelman, 2006; Kowal et al., 2017a; Kowal, 2018). Details on the construction of $\mathbf{b}(\cdot)$ and $\mathbf{\Omega}$ are given in Kowal (2018).

We construct a Bayesian backfitting sampling algorithm that iteratively draws from the full conditional distribution of $\boldsymbol{\psi}_k$ conditional on $\{\boldsymbol{\psi}_\ell\}_{\ell \neq k}$, which is known in closed form, and set $\mathbf{f}_k = \mathbf{B}\boldsymbol{\psi}_k$ for basis matrix $\mathbf{B} = (\mathbf{b}(\tau_1), \dots, \mathbf{b}(\tau_m))'$ (see Appendix). During sampling, we enforce the matrix orthonormality constraint $\mathbf{F}'\mathbf{F} = \mathbf{I}_K$, where $\mathbf{F} = (\mathbf{f}_1, \dots, \mathbf{f}_K)$ and \mathbf{I}_K is the $K \times K$ identity matrix. This constraint, combined with the ordering constraint on $k = 1, \dots, K$ implied by the MGP prior, is sufficient for identifiability (up to sign changes, which in our experience are not problematic in the MCMC sampler). For each k , the orthonormality constraint is enforced by (i) conditioning on the *linear* orthogonality constraints $\mathbf{f}'_k \mathbf{f}_\ell = 0$ for $\ell \neq k$ and (ii) rescaling \mathbf{f}_k to unit norm (see Appendix). As a result, $\mathbf{F}'\mathbf{F} = \mathbf{I}_K$ is satisfied for *every* MCMC iteration, which is necessary for the sampling approach in Section 3. The computational complexity of the sampling algorithm depends on the number of basis functions L_m rather than the number of observation points m . If each f_k is smooth, we may let $L_m \ll m$ to improve scalability without sacrificing model fit; if f_k is non-smooth, other basis functions such as wavelets may be more appropriate.

3 An Efficient Sampler for the Regression Coefficients

We leverage the matrix orthonormality constraints in Section 2.3 to produce improvements in computational efficiency for the MCMC sampling algorithm. These computational gains are essential for moderate to large number of predictors p , and produce algorithms for fully Bayesian inference that are empirically faster than existing alternatives. In addition, matrix orthonormality often corresponds to superior MCMC efficiency in regression (Gilks et al., 1995) and functional data analysis (Crainiceanu and Goldsmith, 2010).

The matrix orthonormality constraint $\mathbf{F}'\mathbf{F} = \mathbf{I}_K$ is enforced at every MCMC iteration,

and provides a simplified likelihood for the model parameters in (2):

Lemma 1. *Under the constraint $\mathbf{F}'\mathbf{F} = \mathbf{I}_K$, the joint likelihood in (7) for $\{\beta_{k,i}\}$ is equivalent to the working likelihood implied by*

$$y_{k,i} = \beta_{k,i} + e_{k,i}, \quad e_{k,i} \stackrel{\text{indep}}{\sim} N(0, \sigma_\epsilon^2) \quad (8)$$

up to a constant that does not depend on $\beta_{k,i}$, where $y_{k,i} = \mathbf{f}'_k \mathbf{Y}_i$ and $e_{k,i} = \mathbf{f}'_k \boldsymbol{\epsilon}_i$.

The utility of Lemma 1 is that, for sampling the parameters in (2) which depend on $\beta_{k,i}$, we may replace the functional data likelihood (7) with the simple likelihood (8). Note that computation of the *projected data* $y_{k,i} = \mathbf{f}'_k \mathbf{Y}_i$ is a one-time cost per MCMC iteration.

Given the likelihood (8) with (2)-(3), we construct an efficient sampler for the regression parameters $\{\mu_k, \alpha_{j,k}, \gamma_{k,i}\}$ using state-of-the-art algorithms for Bayesian linear regression. We sample the regression parameters $\{\mu_k, \alpha_{j,k}, \gamma_{k,i}\}_{j,k,i}$ jointly, which improves MCMC efficiency, and is a common strategy in Bayesian mixed effects models. Sampling from the full conditional distribution of $[\{\mu_k, \alpha_{j,k}, \gamma_{k,i}\} | \mathbf{Y}, \dots]$ is accomplished in two steps: (i) sample the regression coefficients $\{\mu_k, \alpha_{j,k}\}$ after marginalizing over the subject-specific effects $\{\gamma_{k,i}\}$, and (ii) sample $\{\gamma_{k,i}\}$ conditional on $\{\mu_k, \alpha_{j,k}\}$. The relevant full conditional distributions are given in the Appendix. A key feature of the proposed sampling strategy is that both component samplers (i) and (ii) are efficient. For the regression sampler (i), we apply Rue (2001) when $p < n$ with computational complexity $\mathcal{O}(p^3)$ and Bhattacharya et al. (2016) when $p > n$ with computational complexity $\mathcal{O}(n^2p)$. The Bhattacharya et al. (2016) sampler is designed for high dimensional Bayesian regression, but to the best of our knowledge has not been incorporated into Bayesian functional regression. The subject-specific effects sampler (ii) has computational complexity $\mathcal{O}(nK)$ for all $\{\gamma_{k,i}\}$, which allows us to incorporate subject-specific functional effects, modeled nonparametrically in τ via $\{f_k\}$, with minimal additional computational cost. In totality, the algorithm scales linearly in either p or n .

In Figure 1, we present empirical computing times for the proposed algorithm (*FOSR).

For comparison with existing frequentist and Bayesian methods for FOSR, we include Reiss et al. (2010), which uses a generalized least squares estimation procedure (refund:GLS), and Goldsmith and Kitago (2016), which constructs a Gibbs sampler for a Bayesian FOSR model (refund:Gibbs), both implemented in the `refund` package in R (Goldsmith et al., 2016). The `refund` implementations require $p < n$. Figure 1 demonstrates that the proposed algorithm is fast, scalable, and superior to Bayesian and frequentist alternatives, and empirically validates linear time complexity in either p or n . A group lasso alternative (Barber et al., 2017) was also considered, but omitted from Figure 1 since it was noncompetitive.

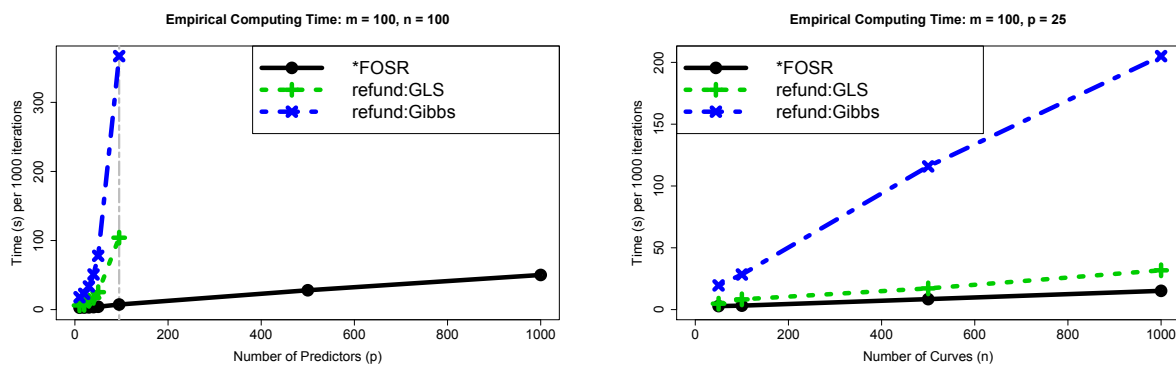


Figure 1: Empirical computing time for several FOSR algorithms with varying p (**left**) and varying n (**right**) reported in seconds per 1000 MCMC iterations for Bayesian methods and total computing time for frequentist methods (using R on a MacBook Pro, 2.7 GHz Intel Core i5). Each computing time is an average of 10 replicates. The vertical gray dashed line (left) indicates $p = 95$, for which *FOSR runs in about 7 seconds. The proposed algorithm is empirically faster, with linear time complexity in either p or n .

4 Decoupling Shrinkage and Selection for Functional Data

Variable selection is a fundamental component in regression problems, including FOSR. For Bayesian regression with a moderate to large p , the regression coefficients are commonly endowed with a sparsity prior, such as the spike-and-slab prior (e.g., Mitchell and Beauchamp, 1988; George and McCulloch, 1997), or a shrinkage prior (e.g., Polson and Scott, 2010; Carvalho et al., 2010). Regardless of the choice of prior, selecting variables based on the joint posterior distribution of the regression coefficients remains a significant challenge. A detailed

discussion of variable selection is beyond the scope of this article; see O’Hara and Sillanpää (2009); Hahn and Carvalho (2015) and the references therein.

Hahn and Carvalho (2015) reframe the Bayesian variable selection problem as a *posterior summarization* problem: using the posterior distribution of the regression coefficients, how can we select a sparse subset of predictors that maintains nearly the predictive ability of the full model? The tradeoff between sparsity and prediction is determined by a loss function, and the variables are selected by optimizing the expected loss under the posterior predictive distribution. By *decoupling shrinkage and selection* (DSS), Hahn and Carvalho (2015) incorporate variable selection (or sparsity) into a variety of models and settings, including multiple linear regression, logistic regression, and Gaussian graphical models, without modifying the models or the accompanying priors. Importantly, unlike popular *marginal* selection approaches, such as the median probability model for sparsity priors (e.g., Barbieri et al., 2004) or hard-thresholding for shrinkage priors (e.g., Ishwaran and Rao, 2005; Carvalho et al., 2010), DSS selects variables *jointly*, while accounting for collinearity among predictors. The generality of the DSS framework suggests that its utility extends far beyond the proposed FOSR model (1)-(3), and may be a useful tool for existing and future Bayesian functional regression models.

4.1 Variable Selection for Function-on-Scalars Regression

We extend the DSS approach of Hahn and Carvalho (2015) to the functional data setting under the general FOSR model (4). Variable selection in this context requires a notion of group sparsity: removing the j th predictor is equivalent to setting $\tilde{\alpha}_j(\tau) = 0$ for *all* $\tau \in \mathcal{T}$. As for scalar responses, the goal here is to identify a small subset of predictors that retains most of the predictive accuracy of the full model. We present a general approach for FOSR below and consider the special case of the reduced-rank model (1) in Section 4.2.

Consider predicting new observations $\tilde{Y}_i(\tau_\ell)$ for each subject $i = 1, \dots, n$ for a pre-defined set of points $\{\tau_\ell\}_{\ell=1}^m$ and design points $\tilde{\mathbf{x}}_i = (\tilde{x}_{i,1}, \dots, \tilde{x}_{i,p})'$, which may differ from $\{x_{i,j}\}_{j=1}^p$.

We propose the following loss function, which combines predictive performance and sparsity:

$$\mathcal{L}(\tilde{\mathbf{Y}}, \tilde{\Delta}) = \frac{1}{nm} \sum_{i=1}^n \|\tilde{\mathbf{Y}}_i - \tilde{\boldsymbol{\delta}}_0 - \tilde{\Delta} \tilde{\mathbf{x}}_i\|_2^2 + \lambda \|\tilde{\Delta}\|_0 \quad (9)$$

where $\|\cdot\|_2$ is the Euclidean norm, $\tilde{\mathbf{Y}}_i = (\tilde{Y}_i(\tau_1), \dots, \tilde{Y}_i(\tau_m))'$, $\tilde{\boldsymbol{\delta}}_0 = (\tilde{\delta}_0(\tau_1), \dots, \tilde{\delta}_0(\tau_m))$ is a functional intercept, $\tilde{\Delta}$ is the $m \times p$ matrix with entries $(\tilde{\Delta})_{\ell,j} = \tilde{\delta}_j(\tau_\ell)$ for regression functions $\tilde{\delta}_j(\cdot)$, and $\|\tilde{\Delta}\|_0 = \sum_{j=1}^p \mathbb{I}\{\tilde{\delta}_j(\tau_\ell) \neq 0 \text{ for some } \ell = 1, \dots, m\}$. The predictive ability of the regression functions $\tilde{\delta}_j(\cdot)$ is measured by the squared prediction error over all points τ_1, \dots, τ_m and subjects $i = 1, \dots, n$, while the second term in (9) encourages column-wise sparsity of $\tilde{\Delta}$, with the tradeoff determined by $\lambda > 0$. An alternative approach is to use the squared L^2 -norm $\|Y\|_{L^2}^2 = \int Y^2(\tau) d\tau$ in place of the squared Euclidean norm in (9). However, the L^2 -norm does not yield the important computational improvements in Section 4.2, and is approximately equivalent to the proposed approach for a fine grid of points $\{\tau_\ell\}$.

To select predictors, we minimize the expectation of the loss function (9) under the posterior predictive distribution, $[\tilde{\mathbf{Y}}|\mathbf{Y}]$, which marginalizes over model parameters, say $\boldsymbol{\theta}$. Although $[\tilde{\mathbf{Y}}|\mathbf{Y}]$ is unavailable in closed form, the conditional predictive distribution $[\tilde{\mathbf{Y}}|\boldsymbol{\theta}]$ and the posterior distribution of the model parameters $[\boldsymbol{\theta}|\mathbf{Y}]$ are sufficient for obtaining a useful representation of the posterior predictive expected loss. The following theorem provides this representation in a more general setting:

Theorem 1. *Define $p_{\text{pred}}(\tilde{\mathbf{Y}}|\mathbf{Y}) = \int p_{\text{like}}(\tilde{\mathbf{Y}}|\boldsymbol{\theta}) p_{\text{post}}(\boldsymbol{\theta}|\mathbf{Y}) d\boldsymbol{\theta}$ to be the posterior predictive distribution with model parameters $\boldsymbol{\theta}$. For known functions $h(\cdot)$ and $g(\cdot)$ mapping to the same co-domain with $\mathbb{E}_{[\tilde{\mathbf{Y}}|\mathbf{Y}]} \|h(\tilde{\mathbf{Y}})\|_2^2 < \infty$, the posterior predictive expectation is*

$$\mathbb{E}_{[\tilde{\mathbf{Y}}|\mathbf{Y}]} \|h(\tilde{\mathbf{Y}}) - g(\tilde{\Delta}; \tilde{\mathbf{x}})\|_2^2 = \|\bar{h} - g(\tilde{\Delta}; \tilde{\mathbf{x}})\|_2^2 \quad (10)$$

up to constants that do not depend on $\tilde{\Delta}$, where $\bar{h} = \mathbb{E}_{[\boldsymbol{\theta}|\mathbf{Y}]}(\hat{h}_\theta)$ is the posterior expectation of $\hat{h}_\theta = \mathbb{E}_{[\tilde{\mathbf{Y}}|\boldsymbol{\theta}]} h(\tilde{\mathbf{Y}})$.

The proof is given in the Appendix. Theorem 1 provides a recipe for computing the minimizer $\tilde{\mathbf{\Delta}}$ of the expected loss (subject to additional penalties on $\tilde{\mathbf{\Delta}}$): use the squared norm on the right hand side of (10), which only requires computation of \bar{h} from the posterior. If the quantity \hat{h}_θ is available analytically, as for multiple linear regression and FOSR with $h(y) = y$ the identity function, then computing the MCMC sample mean of \hat{h}_θ over the posterior draws of $\boldsymbol{\theta}$ will provide an estimate. If \hat{h}_θ is not available, but it is possible to draw from the full conditional predictive distribution $\tilde{\mathbf{Y}}^s \sim [\tilde{\mathbf{Y}}|\boldsymbol{\theta} = \boldsymbol{\theta}^s]$ for posterior sample $s = 1, \dots, S$, then the estimator $S^{-1} \sum_{s=1}^S h(\tilde{\mathbf{Y}}^s)$ will suffice.

For the general FOSR model (4), the *conditional* predictive distribution for $\tilde{\mathbf{Y}}_i$, after marginalizing over the subject-specific effects $\tilde{\gamma}_i(\cdot)$, is $[\tilde{\mathbf{Y}}_i|\boldsymbol{\theta}] \stackrel{indep}{\sim} N(\tilde{\boldsymbol{\mu}} + \tilde{\mathbf{A}}\tilde{\mathbf{x}}_i, \boldsymbol{\Sigma}_i)$, where $\boldsymbol{\theta} = (\tilde{\boldsymbol{\mu}}, \{\tilde{\alpha}_j\}, \{\sigma_{\gamma_{k,i}}\}, \{f_k\}, \sigma_\epsilon)$ are the relevant model parameters, $\tilde{\boldsymbol{\mu}} = (\tilde{\mu}(\tau_1), \dots, \tilde{\mu}(\tau_m))'$, $\tilde{\mathbf{A}}$ is the $m \times p$ matrix with entries $(\tilde{\mathbf{A}})_{\ell,j} = \tilde{\alpha}_j(\tau_\ell)$, and $\boldsymbol{\Sigma}_i = \sigma_\epsilon^2 \mathbf{I}_m + \mathbf{F}\boldsymbol{\Sigma}_{\gamma_i}\mathbf{F}'$ with $\boldsymbol{\Sigma}_{\gamma_i} = \text{diag}(\{\sigma_{\gamma_{k,i}}^2\}_{k=1}^K)$. The form of the conditional predictive distribution is quite general for FOSR; the special case of the proposed model arises in the definition of $\boldsymbol{\Sigma}_i$.

Using Theorem 1 and the conditional predictive distribution above, we may derive a convenient simplification for FOSR:

Corollary 1. *The posterior predictive expectation of the loss in (9) is*

$$\mathbb{E}_{[\tilde{\mathbf{Y}}|\mathbf{Y}]} \mathcal{L}(\tilde{\mathbf{Y}}, \tilde{\mathbf{\Delta}}) = \frac{1}{nm} \sum_{i=1}^n \left\| \left(\tilde{\boldsymbol{\mu}} + \tilde{\mathbf{A}}\tilde{\mathbf{x}}_i \right) - \left(\tilde{\boldsymbol{\delta}}_0 + \tilde{\mathbf{\Delta}}\tilde{\mathbf{x}}_i \right) \right\|_2^2 + \lambda \|\tilde{\mathbf{\Delta}}\|_0 \quad (11)$$

up to constants that do not depend on $\tilde{\boldsymbol{\delta}}_0$ and $\tilde{\mathbf{\Delta}}$, where $\tilde{\boldsymbol{\mu}} = \mathbb{E}[\tilde{\boldsymbol{\mu}}|\mathbf{Y}]$ and $\tilde{\mathbf{A}} = \mathbb{E}[\tilde{\mathbf{A}}|\mathbf{Y}]$.

The posterior predictive expected loss for FOSR is given by (11), which is a penalized regression with response $\tilde{\boldsymbol{\mu}} + \tilde{\mathbf{A}}\tilde{\mathbf{x}}_i$ constructed from posterior expectations and a sparsity penalty on $\tilde{\mathbf{\Delta}}$. For computational tractability, we may replace the penalty $\|\tilde{\mathbf{\Delta}}\|_0$ with a convex relaxation: $\|\tilde{\mathbf{\Delta}}\|_1 = \sum_{j=1}^p \sqrt{m} \|\tilde{\boldsymbol{\Delta}}_j\|_2$ for $\tilde{\boldsymbol{\Delta}}_j = (\tilde{\delta}_j(\tau_1), \dots, \tilde{\delta}_j(\tau_m))'$, which corresponds to the group lasso penalty (Yuan and Lin, 2006). To avoid overshrinkage, we use the following

adaptive group lasso penalty:

$$\|\tilde{\Delta}\|_{1^*} = \sum_{j=1}^p w_j \|\tilde{\Delta}_j\|_2 \quad (12)$$

with weights $w_j = 1/\|\tilde{\mathbf{A}}_j\|_2$ for $\tilde{\mathbf{A}}_j$ the posterior mean of $[\tilde{\alpha}_j(\tau_\ell)]_{\ell=1}^m$. The use of the adaptive group lasso is analogous to the use of the adaptive lasso in Hahn and Carvalho (2015), which demonstrates good performance. The solution path of (11) with modified penalty (12) may be computed using existing software, such as the `gglasso` package in R (Yang and Zou, 2017). Selection of λ is described in Section 4.3.

4.2 Variable Selection for Reduced-Rank Function-on-Scalars Regression

The general approach of Section 4.1 is computationally intensive: the optimization problem (11) contains m terms $\tilde{\delta}_j(\tau_1), \dots, \tilde{\delta}_j(\tau_m)$ for each predictor $j = 1, \dots, p$, where both m and p may be large. Notably, (11) ignores the reduced-rank model structure of (1), which is designed for parsimonious modeling and computational efficiency. In particular, the response variable in the penalized regression problem (11) is $\tilde{\boldsymbol{\mu}} + \tilde{\mathbf{A}}\tilde{\mathbf{x}}_i = \mathbb{E}[\mathbf{F}\boldsymbol{\mu} + \mathbf{F}\mathbf{A}\tilde{\mathbf{x}}_i|\mathbf{Y}]$ for $\boldsymbol{\mu} = (\mu_1, \dots, \mu_K)'$ and $(\mathbf{A})_{k,j} = \alpha_{j,k}$, which is the posterior expectation of a reduced-rank matrix.

To exploit the model structure of (1), suppose each DSS regression function is a linear combination of the loading curves: $\tilde{\delta}_j(\tau) = \sum_{k=1}^K f_k(\tau)\delta_{j,k}$ for $j = 1, \dots, p$. This definition reflects the connection between (1)-(3) and (4)-(5). Now, the condition $\delta_{j,k} = 0$ for $k = 1, \dots, K$ is sufficient (and necessary) for the previous notion of sparsity, $\tilde{\delta}_j(\tau) = 0$ for all $\tau \in \mathcal{T}$. Therefore, we may conduct group selection in a K -dimensional space instead of an m -dimensional space, with $K \ll m$. The resulting algorithm is substantially faster than the general approach in Section 4.1—which for large m or large p may not be feasible—and uniquely capitalizes on the features of the proposed model.

The expansion $\tilde{\delta}_j(\tau) = \sum_{k=1}^K f_k(\tau)\delta_{j,k}$ presents a new challenge: unlike the loss function in (9), any loss function involving $\tilde{\delta}_j(\cdot)$ now depends on the model parameters $\{f_k\}$. However, the $\{f_k\}$ are unknown, and the accompanying uncertainty cannot be ignored. We propose

to construct an *expected* loss function directly by integrating over \mathbf{F} :

$$\mathcal{E}\mathcal{L}(\Delta) = \mathbb{E}_{[\mathbf{F}|\mathbf{Y}]} \left\{ \mathbb{E}_{[\tilde{\mathbf{Y}}|\mathbf{F},\mathbf{Y}]} \left[\frac{1}{nm} \sum_{i=1}^n \|\tilde{\mathbf{Y}}_i - \mathbf{F}\delta_0 - \mathbf{F}\Delta\tilde{\mathbf{x}}_i\|_2^2 + \lambda\|\Delta\|_0 \right] \right\} \quad (13)$$

where $\delta_0 = (\delta_{0,1}, \dots, \delta_{0,K})$ is a K -dimensional intercept, Δ is the $K \times p$ matrix with entries $(\Delta)_{k,j} = \delta_{j,k}$, and $\|\Delta\|_0 = \sum_{j=1}^p \mathbb{I}\{\delta_{j,k} \neq 0 \text{ for some } k = 1, \dots, K\}$. The term in square brackets in (13) is identical to (9) under the assumptions $\tilde{\delta}_0 = \mathbf{F}\delta_0$ and $\tilde{\Delta} = \mathbf{F}\Delta$, similar to a sparse reduced-rank regression model (Chen and Huang, 2012). The additional complexity in (13) is due to the uncertainty of $\{f_k\}$, which requires successive averaging over the distributions $[\tilde{\mathbf{Y}}|\mathbf{F}, \mathbf{Y}]$ and $[\mathbf{F}|\mathbf{Y}]$ to obtain the posterior predictive expectation under $[\tilde{\mathbf{Y}}|\mathbf{Y}]$. Note that in general, $[\tilde{\mathbf{Y}}|\mathbf{F}, \mathbf{Y}]$ is not equal to $[\tilde{\mathbf{Y}}|\mathbf{F}]$: while it is often assumed that $\tilde{\mathbf{Y}}$ is conditionally independent of \mathbf{Y} given *all* model parameters, this distribution is only conditional on \mathbf{F} . An important special case of (13) is when \mathbf{F} is known, e.g., $\mathbf{F} = \mathbf{B}$ is a matrix of splines, which implies $\mathcal{E}\mathcal{L}(\Delta) = \mathbb{E}_{[\tilde{\mathbf{Y}}|\mathbf{Y}]} \mathcal{L}(\tilde{\mathbf{Y}}, \tilde{\Delta})$ for $\tilde{\delta}_0 = \mathbf{F}\delta_0$ and $\tilde{\Delta} = \mathbf{F}\Delta$.

We derive a convenient representation of (13):

Theorem 2. *Under the orthonormality constraint $\mathbf{F}'\mathbf{F} = \mathbf{I}_K$,*

$$\mathcal{E}\mathcal{L}(\Delta) = \frac{1}{nm} \sum_{i=1}^n \left\| (\bar{\boldsymbol{\mu}} + \bar{\mathbf{A}}\tilde{\mathbf{x}}_i) - (\boldsymbol{\delta}_0 + \Delta\tilde{\mathbf{x}}_i) \right\|_2^2 + \lambda\|\Delta\|_0 \quad (14)$$

up to constants that do not depend on $\boldsymbol{\delta}_0$ and Δ , where $\bar{\boldsymbol{\mu}} = \mathbb{E}[\boldsymbol{\mu}|\mathbf{Y}]$ and $\bar{\mathbf{A}} = \mathbb{E}[\mathbf{A}|\mathbf{Y}]$ for $\boldsymbol{\mu} = (\mu_1, \dots, \mu_K)'$ and $(\mathbf{A})_{k,j} = \alpha_{j,k}$.

The proof is in the Appendix. Analogous to Corollary 1, the posterior predictive expected loss is a penalized regression with response vector $\bar{\boldsymbol{\mu}} + \bar{\mathbf{A}}\tilde{\mathbf{x}}_i$ and a sparsity penalty on Δ . In this case, however, the response vector is K -dimensional instead of m -dimensional, and the sparsity penalty operates in a K -dimensional space instead of an m -dimensional space, with $K \ll m$. We again replace the penalty $\|\Delta\|_0$ with a more tractable convex relaxation: $\|\Delta\|_1 = \sum_{j=1}^p \sqrt{K}\|\Delta_j\|_2$ for $\Delta_j = (\delta_{j,1}, \dots, \delta_{j,K})'$. An adaptive group lasso penalty may be

used to avoid overshrinkage, as in (12): $\|\Delta\|_{1^*} = \sum_{j=1}^p w_j \|\Delta_j\|_2$ with weights $w_j = 1/\|\bar{\mathbf{A}}_j\|_2$ for $\bar{\mathbf{A}}_j$ the posterior mean of $(\alpha_{j,1}, \dots, \alpha_{j,K})'$.

Given a solution $\hat{\Delta}$ to (14) using the aforementioned convex relaxation, the DSS estimator of the regression functions is $\mathbb{E}[\mathbf{F}\hat{\Delta}|\mathbf{Y}] = \bar{\mathbf{F}}\hat{\Delta}$ where $\bar{\mathbf{F}} = \mathbb{E}[\mathbf{F}|\mathbf{Y}]$ is the posterior expectation of the loading curve matrix.

4.3 Selection Summary Plots

The DSS posterior summarization approaches of Sections 4.1 and 4.2 result in the penalized regression problems (11) and (14), respectively, both of which depend on a tuning parameter $\lambda > 0$. We select λ using proportion of variability explained in the FOSR model, analogous to Hahn and Carvalho (2015), by identifying a sparsified model for which the predictive ability is within a reasonable range of uncertainty of the predictive ability of the full model.

Consider the following notion of proportion of variability explained at design points $\{\tilde{x}_{i,j}\}$, analogous to R^2 in linear regression:

$$\rho^2 = \frac{\|\mathbf{A}\tilde{\mathbf{X}}'\|_F^2}{\mathbb{E}_{[\tilde{\mathbf{Y}}|\theta]} \|\tilde{\mathbf{Y}}\|_F^2} = \frac{\|\mathbf{A}\tilde{\mathbf{X}}'\|_F^2}{\|\mathbf{A}\tilde{\mathbf{X}}'\|_F^2 + \sum_{i=1}^n \text{tr}(\boldsymbol{\Sigma}_i)} \quad (15)$$

where $\tilde{\mathbf{X}}$ is the $n \times p$ matrix of predictors $[\tilde{x}_{i,j}]_{i,j}$, $\tilde{\mathbf{Y}}$ is the $n \times m$ matrix of predictive values $[\tilde{Y}_i(\tau_\ell)]_{i,\ell}$, $\|\cdot\|_F$ denotes the Frobenius norm, and $\text{tr}(\cdot)$ is the trace operator. Equation (15) may be simplified, since $\sum_{i=1}^n \text{tr}(\boldsymbol{\Sigma}_i) = nm\sigma_\epsilon^2 + \sum_{i=1}^n \sum_{k=1}^K \sigma_{\gamma_{k,i}}^2$. This decomposition is informative: the total variance in the denominator of (15) includes the regression model term $\mathbf{A}\tilde{\mathbf{X}}'$, the observation error variance σ_ϵ^2 , and the subject-specific variances $\sigma_{\gamma_{k,i}}^2$. Note that the intercept is excluded from (15), but this is not strictly necessary. We use the $K \times p$ matrix \mathbf{A} to define ρ^2 (and ρ_λ^2 below), but substituting the $m \times p$ matrix $\tilde{\mathbf{A}} = \mathbf{F}\mathbf{A}$ in (15) (or (16) below) produces an identical definition due to the orthonormality of \mathbf{F} .

For a given tuning parameter λ , let Δ_λ denote the solution to (14) with the adaptive group lasso penalty. Model discrepancy, due to re-estimation under sparsity, contributes to

total variance:

$$\rho_\lambda^2 = \frac{\|\mathbf{A}\tilde{\mathbf{X}}'\|_F^2}{\mathbb{E}_{[\tilde{\mathbf{Y}}|\boldsymbol{\theta}]} \|\tilde{\mathbf{Y}}\|_F^2 + \|\mathbf{A}\tilde{\mathbf{X}}' - \boldsymbol{\Delta}_\lambda \tilde{\mathbf{X}}'\|_F^2} \quad (16)$$

which we may simplify as above using $\mathbb{E}_{[\tilde{\mathbf{Y}}|\boldsymbol{\theta}]} \|\tilde{\mathbf{Y}}\|_F^2 = \|\mathbf{A}\tilde{\mathbf{X}}'\|_F^2 + nm\sigma_\epsilon^2 + \sum_{i=1}^n \sum_{k=1}^K \sigma_{\gamma_{k,i}}^2$. Note that $\lambda = 0$ implies $\boldsymbol{\Delta}_{\lambda=0} = \bar{\mathbf{A}}$ is the posterior mean and $\rho_{\lambda=0}^2 = \rho^2$.

Since ρ^2 and ρ_λ^2 are functions of model parameters $\boldsymbol{\theta}$, we may compare their respective posterior distributions to assess disparities in predictive ability among sparsified models. We construct a posterior selection summary plot as follows: (i) using the `gglasso` package in R (Yang and Zou, 2017), minimize (14) with the adaptive group lasso penalty for $\boldsymbol{\Delta}_\lambda$ on a grid of λ values; (ii) for each $\boldsymbol{\Delta}_\lambda$, compute the posterior distribution of ρ_λ^2 by substituting the posterior draws of \mathbf{A} , σ_ϵ , and $\sigma_{\gamma_{k,i}}$ into (16); and (iii) plot the expected value and 90% credible intervals of ρ_λ^2 against model size $\|\boldsymbol{\Delta}_\lambda\|_0$. The resulting plot shows how predictive ability declines with sparsity, but importantly includes the accompanying uncertainty. For an example, see Figure 4. As a general guideline for model selection, we choose the smallest model for which the 90% posterior credible interval for ρ_λ^2 contains $\mathbb{E}[\rho^2|\mathbf{Y}]$.

5 Simulations

5.1 Simulation Design

A simulation study was conducted in order to (i) compare the estimation accuracy of the proposed method against existing alternatives, (ii) evaluate posterior uncertainty quantification among Bayesian FOSR models, and (iii) study the variable selection properties of the proposed DSS procedure. We are primarily interested in how these properties vary in the number of predictors, so we consider $p \in \{20, 50, 500\}$ with fixed $p_1 = 10$ non-null predictors. All simulations use $n = 100$ curves with $m = 30$ equally-spaced points in $[0, 1]$.

For each subject i , we simulated correlated predictors $\{x_{i,j}\}_{j=1}^p$ from a normal distribution with mean zero and covariance $\text{Cov}(x_{i,j}, x_{i,j'}) = 0.75^{|j-j'|}$, with $p_1 = 10$ non-null predictors

evenly-spaced from $1, \dots, p$. Functional observations are simulated based on model (1)-(2). For the true loading curves, we set $f_1^*(\tau) = 1/\sqrt{m}$ and for $k = 2, \dots, K^* = 4$, we let f_k^* be an orthogonal polynomial of degree k . For each non-null predictor j , we uniformly sample K_j^* factors to be nonzero, where K_j^* follows a Poisson(1) distribution truncated to $[1, K^*]$, and draw the nonzero factor coefficients $\alpha_{j,k}^* \stackrel{\text{indep}}{\sim} N(0, 1/k^2)$. As a result, each non-null predictor j may be associated with the functional response via a subset of $\{f_k^*\}_{k=1}^{K^*}$. We simulate the true factors $\beta_{k,i}^* = \mu_k^* + \sum_{j=1}^p x_{j,i} \alpha_{j,k}^* + \gamma_{k,i}^*$, where $\mu_k^* = 1/k$ and $\gamma_{k,i}^* \stackrel{\text{indep}}{\sim} N(0, 1/k^2)$, which incorporates subject-specific random effects. Based on the true curves $Y_i^*(\tau) = \sum_{k=1}^{K^*} f_k^*(\tau) \beta_{k,i}^*$, the functional observations are $Y_i(\tau) = Y_i^*(\tau) + \sigma^* \epsilon_i^*(\tau)$, where $\epsilon_i^*(\tau) \stackrel{\text{iid}}{\sim} N(0, 1)$. The observation error standard deviation σ^* is determined by the *root-signal-to-noise ratio* (RSNR): $\sigma^* = \sqrt{\frac{\sum_{i=1}^n \sum_{j=1}^m (Y_i^*(\tau_j) - \bar{Y}^*)^2}{nm-1}} / \text{RSNR}$ where \bar{Y}^* is the sample mean of $\{Y_i^*(\tau_j)\}_{j,i}$. We select RNSR = 5 for moderately noisy functional data.

5.2 Methods For Comparison

We implement the proposed model (1)-(3) with the shrinkage priors and loading curves of Sections 2.2 and 2.3, respectively, with $K = 6 > K^* = 4$ (*FOSR). Using this posterior distribution, we compute the sparse DSS estimates from Section 4.2 (*FOSR-DSS). For comparison with *FOSR-DSS, we also select variables marginally using GBPVs, which retain a variable j if the simultaneous credible bands for $\{\tilde{\alpha}_j(\tau_\ell)\}_{\ell=1}^m$ exclude zero for some τ_ℓ .

We include two variations of (1)-(3) based on alternative models for $\{f_k\}$: Basis-FPCA, which estimates $\{f_k\}$ as FPCs using Xiao et al. (2013) with the number of FPCs selected to explain 99% of the variability in $\{Y_i(\tau_\ell) - \bar{Y}(\tau_\ell)\}_{\ell,i}$, and Basis-Spline, which uses an (orthonormalized) LR-TPS basis for $\{f_k\}$. Both Basis-FPCA and Basis-Spline use normal-inverse-gamma priors for (3). Importantly, Basis-FPCA and Basis-Spline provide baselines for assessing the potential gains in point estimation and uncertainty quantification associated with the proposed shrinkage priors and the model for $\{f_k\}$. Basis-FPCA and Basis-Spline are implemented using the proposed Gibbs sampler (see Appendix) by omitting the loading

curve sampling step, and rely on the computational results of Section 3 for scalability.

Lastly, we include three FOSR methods from the `refund` package in R (see Figure 1): estimation with a group lasso for variable selection (`refund:Lasso`; Barber et al., 2017), estimation using generalized least squares (`refund:GLS`; Reiss et al., 2010), and a Bayesian model using FPCs to estimate the residual covariance (`refund:Gibbs`; Goldsmith and Kitago, 2016). Note that for $p = 500$, the `refund` methods are not computationally feasible.

We compare methods using three metrics. For point estimation, we use the root mean square error of the regression coefficient functions, $\text{RMSE} = \sqrt{\frac{1}{pm} \sum_{j=1}^p \sum_{l=1}^m [\tilde{\alpha}_j(\tau_\ell) - \tilde{\alpha}_j^*(\tau_\ell)]^2}$, where $\tilde{\alpha}_j(\tau_\ell)$ is the estimated regression coefficient for predictor j and observation point τ_ℓ and $\tilde{\alpha}_j^*(\tau_\ell) = \sum_{k=1}^{K^*} f_k^*(\tau_\ell) \alpha_{j,k}^*$ is the true regression coefficient. The Bayesian methods use the posterior expectation of $\tilde{\alpha}_j(\tau_\ell)$ as the estimator. For uncertainty quantification among the Bayesian methods, we compute the mean credible interval width for all regression coefficient functions, $\text{MCIW} = \frac{1}{pm} \sum_{j=1}^p \sum_{l=1}^m \left[\tilde{\alpha}_j^{(97.5)}(\tau_\ell) - \tilde{\alpha}_j^{(2.5)}(\tau_\ell) \right]$, where $\tilde{\alpha}_j^{(q)}(\tau_\ell)$ is the $q\%$ quantile of the posterior distribution for $\tilde{\alpha}_j(\tau_\ell)$, along with the empirical coverage probability, $\frac{1}{pm} \sum_{j=1}^p \sum_{l=1}^m \mathbb{I}\{\tilde{\alpha}_j^{(2.5)}(\tau_\ell) \leq \tilde{\alpha}_j^*(\tau_\ell) \leq \tilde{\alpha}_j^{(97.5)}(\tau_\ell)\}$. The goal is to achieve the smallest MCIW with the correct nominal coverage (0.95). For comparing variable selection techniques, we compute receiver-operating characteristic (ROC) curves. ROC curves plot the true positive rate, or sensitivity, against the false positive rate, or $1 - \text{specificity}$, as the decision threshold varies, where a positive predictor corresponds to a non-zero regression function. ROC curves further toward the upper left corner indicate superiority of the method.

5.3 Simulation Results

Figure 2 displays RMSEs and MCIWs for 100 simulated datasets. The RMSEs show that *FOSR provides the best point estimation for all p , with the most substantial improvements for moderate to large $p \geq 50$. The sparse estimates from *FOSR-DSS perform at least as well as `refund:Lasso` for $p = 20$, and are outperformed only by *FOSR for $p \geq 50$. The case of $p = 500$ demonstrates the utility of the shrinkage priors of Section 2.2, as Basis-FPCA

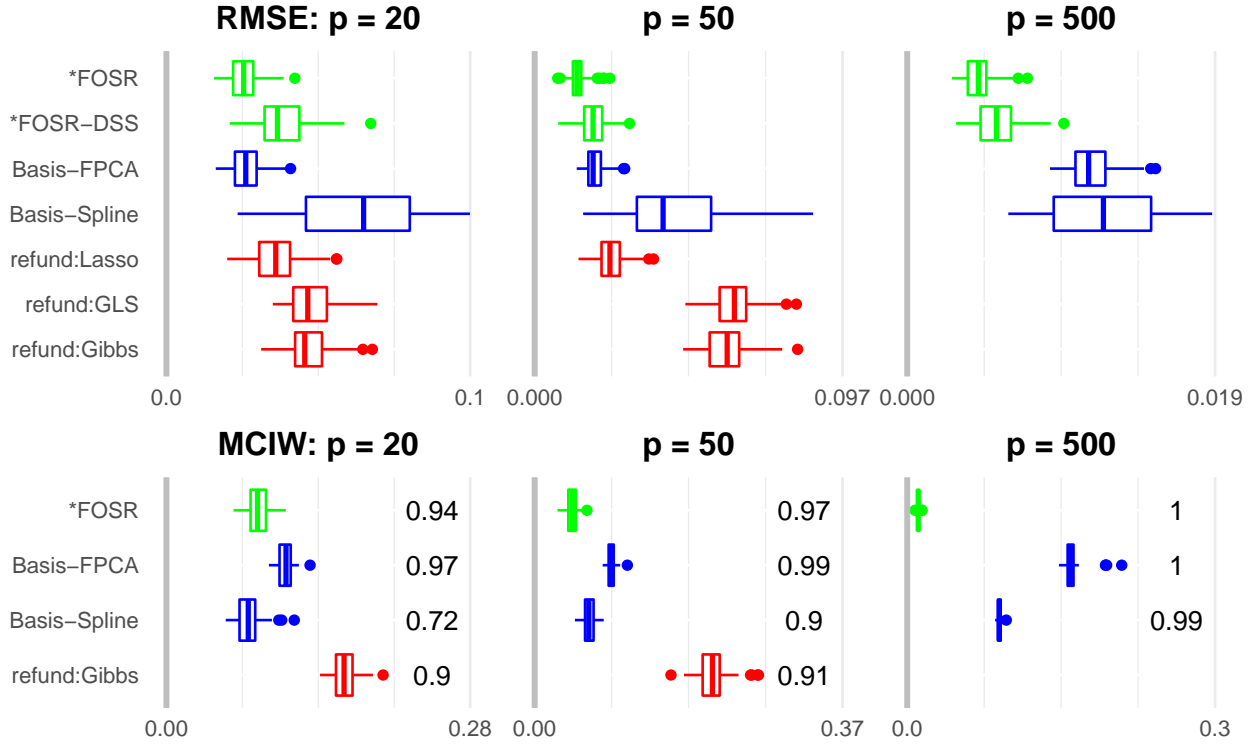


Figure 2: Root mean squared errors (**top row**) and mean 95% credible interval width (MCIW) with empirical coverage probabilities (**bottom row**) for the regression coefficient functions $\tilde{\alpha}_j(\tau)$. The proposed methods (*FOSR and *FOSR-DSS) are in green, the $\{f_k\}$ -modified methods (Basis-FPCA and Basis-Spline) are in blue, and existing methods (refund:Lasso, refund:GLS, and refund:Gibbs) are in red. Existing methods were not feasible for $p = 500 > n = 100$. For display purposes, outliers of Basis-Spline are not shown.

and Basis-Spline are clearly dominated by *FOSR and *FOSR-DSS. Estimation of $\{f_k\}$ is also important: there is a sizable gap for all p between Basis-Spline, which does *not* estimate $\{f_k\}$, and *FOSR, *FOSR-DSS, and Basis-FPCA, which do estimate $\{f_k\}$.

The MCIWs in Figure 2 demonstrate that the proposed *FOSR provides significantly narrower credible intervals than competing Bayesian methods, particularly for $p \geq 50$, while maintaining approximately the correct nominal coverage. Note that although Basis-Spline produces narrow credible intervals, it suffers from substantial undercoverage. The large improvements of *FOSR relative to Basis-FPCA suggest that the proposed shrinkage priors and model for the loading curves—which, unlike Basis-FPCA, accounts for the uncertainty of the unknown $\{f_k\}$ —are both important for more precise uncertainty quantification.

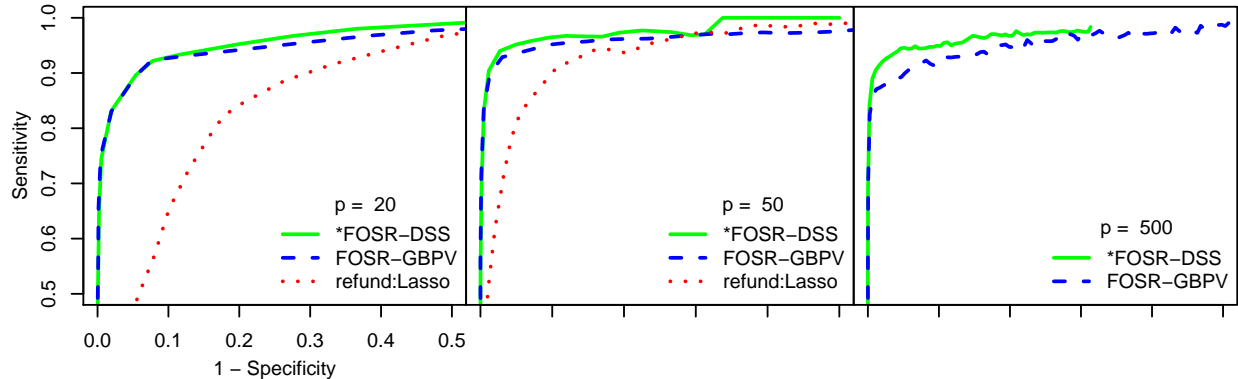


Figure 3: ROC curves to compare variable selection techniques. Each point along the ROC curve is the average sensitivity and $1 - \text{specificity}$ of a given model size. For $p = 500$, *FOSR-DSS selects only a few false positives, so the corresponding ROC curve does not extend to lower (i.e., worse) specificity.

In Figure 3, we show ROC curves for the competing variable selection techniques: *FOSR-DSS, FOSR-GBP, and refund:Lasso. For all p , the proposed *FOSR-DSS is at least as good as the other methods, with greater improvements relative to FOSR-GBP as p increases. Notably, refund:Lasso is inferior to both Bayesian methods for variable selection.

6 Time-of-Day Physical Activity Levels for Elderly Adults

We analyze time-of-day physical activity levels for an elderly population obtained from the National Sleep Research Resource (Dean et al., 2016; Zhang et al., 2018) in conjunction with the Multi-Ethnic Study of Atherosclerosis. The dataset consists of actigraphy measurements and an accompanying sleep questionnaire (see Table 2) for black, white, Hispanic, and Chinese-American men and women. The aim of our investigation was to identify question items from a sleep questionnaire that are predictive of time-of-day physical activity levels, and to estimate and perform inference on these time-of-day effects.

To focus primarily on waking hours, we considered activity levels from 6am to 10pm on Wednesday and Saturdays. The raw count activity data was summed into 20 minute time increments and modeled as a function of time-of-day with $m = 48$ observation points. Days

with more than 10% missingness typically had long periods of no activity recorded and were removed from the analysis. Of the remaining days, 6% had missing observation points, which were imputed automatically within the Gibbs sampler (see Appendix). In total, 2059 people ages 54-95 were considered over a cumulative $n = 3568$ days.

Covariate information included age, gender, race/ethnicity, a Wednesday/Saturday indicator, and questionnaire responses. Due to substantial missingness among questionnaire responses, we chose to model sleep questionnaire items as categorical variables, grouped into high, low, and missing responses where appropriate (see Table 2 and the supplement for details). In total, 34 items from the questionnaire were included and $p = 74$.

Posterior samples from model (1)-(3) with shrinkage priors (Section 2.2) and unknown loading curves (Section 2.3) were obtained using the MCMC sampling algorithm in the Appendix. We report results for $K = 6$; larger values of K produced similar results. Traceplots demonstrate good mixing and suggest convergence (see the supplementary material).

We applied the reduced-rank DSS procedure from Section 4.2 to identify demographic variables and questionnaire items that predict intraday physical activity. We chose to perform DSS on the *category levels* rather than the questionnaire items: selected levels imply inclusion of the corresponding questionnaire item (along with the baseline category), but do not require other levels be included. The selection summary plot in Figure 4 displays the tradeoff between predictive accuracy and sparsity: the proportion of variability explained increases quickly between models of size six and ten, but does not notably increase for larger models. The plot suggests that the most reasonable model size is between eight and ten, while larger models do not offer additional predictive ability. Guided by Figure 4, we select ten predictors: **Saturday**, **Gender**, **age**, and the seven categories of the four questionnaire items in Table 1. Impressively, these four questionnaire items (along with **Saturday**, **Gender**, and **age**) retain nearly the predictive ability of the full questionnaire.

The estimated coefficient functions and 95% simultaneous credible bands for several DSS-selected variables are displayed in Figure 5. Most notably, these effects are time-varying,

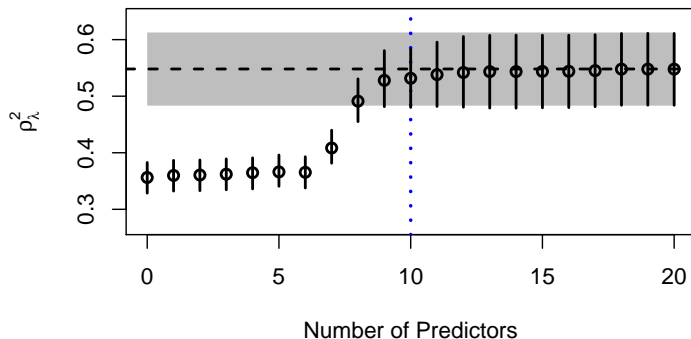


Figure 4: The selection summary plot for the time-of-day physical activity data. Shown is the proportion of variability explained (with 95% credible intervals) for increasing model sizes as selected by DSS. The horizontal line denotes the proportion of variability explained by the full model with the gray band denoting the 95% credible interval. As model size increases, the explanatory power of the model increases. Predictive performance improves substantially from six to ten predictors, but including more than ten predictors offers no further improvement. The vertical blue line denotes the selected model with ten predictors.

Item name	Categories	Question Content
bedtmwkd	missing/ 5-7/8-9 /10-11/ later	Bedtime Weekday
nap	missing/ low /high	Usual Week: Number Of Naps
types	missing/ evening /morning/neither	Type Of Person: Morning Or Evening
wkdaysleepdur	missing/<7/ 7-9 / >9	Sleep duration weekday

Table 1: The questionnaire item name, categories, and question content of the items selected by DSS. The first category in each row is the contrasting variable and the selected categories are in blue and bolded.

which confirms the importance of using a *functional* regression model. The simultaneous credible bands for age are below zero for all times of day, indicating that daily activity declines with age. This effect is largest from 10am to 4pm, which we note is the most active time of day in the study. Individuals who reported frequent napping also tended to be less active throughout the day, particularly in the mid-afternoon. Physical activity levels were lower on Saturday mornings compared to Wednesday mornings, but were similar throughout the rest of the day. Lastly, self-described “evening people” were substantially less active in the morning than “morning people”, but more surprisingly, were also less active overall.

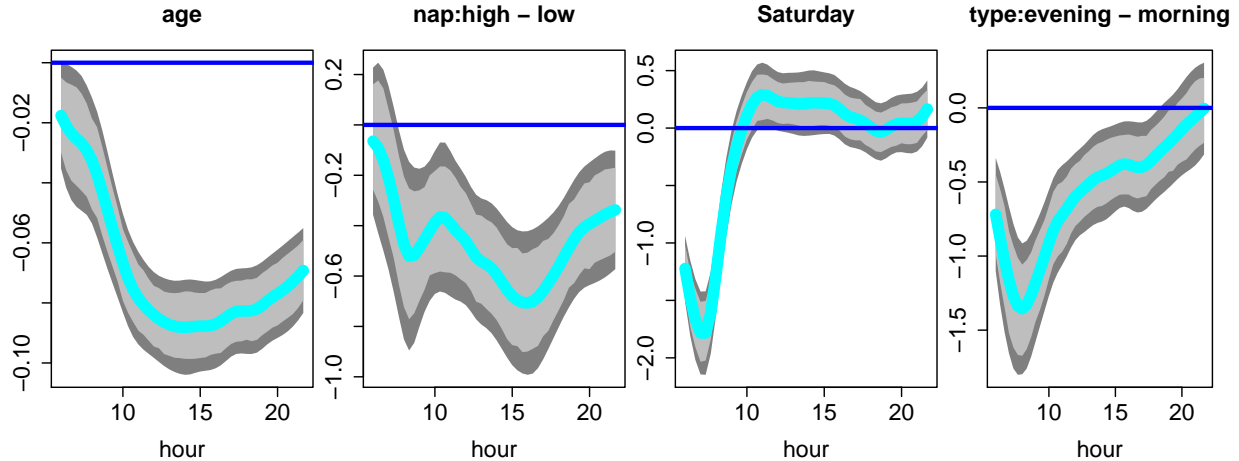


Figure 5: Estimated regression coefficient functions for DSS-selected variables, 95% pointwise credible intervals (light gray), and 95% simultaneous credible bands (dark grey). A horizontal blue line denotes zero change in activity.

7 Conclusions

We developed a fully Bayesian framework for function-on-scalars regression with many predictors. Nonparametric and unknown basis functions were proposed for greater modeling flexibility and proper uncertainty quantification via the posterior distribution. Carefully-designed shrinkage priors were employed to minimize the impact of unimportant predictor variables, which is particularly important for moderate to large p . We introduced a novel variable selection technique for functional regression, which identifies a sparse subset of predictors that minimizes loss in predictive performance relative to the full model. A simulation study illustrated the improvements in point estimation, uncertainty quantification, and variable selection offered by the proposed methodology. Full posterior inference was provided by a highly efficient Gibbs sampler with computational complexity scaling in either n or p . The methodology was applied to an actigraphy and sleep questionnaire dataset from the National Sleep Research Resource.

The proposed methodology offers several promising extensions. Modifications for binomial and count data are available by coupling the computational approach of Section 3 with

well-known Gaussian parameter expansions (e.g., Polson et al., 2013). Alternative models for $\{f_k\}$ may be introduced for other applications, for example wavelets for non-smooth functional data or Fourier basis functions for periodic functional data. Lastly, the proposed DSS approach offers a general framework for Bayesian variable selection and posterior summarization in other functional, spatial, and time series regression problems.

References

- Barber, R. F., Reimherr, M., and Schill, T. (2017). The function-on-scalar LASSO with applications to longitudinal GWAS. *Electronic Journal of Statistics*, 11(1):1351–1389.
- Barbieri, M. M., Berger, J. O., et al. (2004). Optimal predictive model selection. *The Annals of Statistics*, 32(3):870–897.
- Bhattacharya, A., Chakraborty, A., and Mallick, B. K. (2016). Fast sampling with gaussian scale mixture priors in high-dimensional regression. *Biometrika*, 103(4):985–991.
- Bhattacharya, A. and Dunson, D. B. (2011). Sparse Bayesian infinite factor models. *Biometrika*, pages 291–306.
- Brumback, B. A. and Rice, J. A. (1998). Smoothing spline models for the analysis of nested and crossed samples of curves. *Journal of the American Statistical Association*, 93(443):961–976.
- Carvalho, C. M., Polson, N. G., and Scott, J. G. (2010). The horseshoe estimator for sparse signals. *Biometrika*, pages 465–480.
- Chen, L. and Huang, J. Z. (2012). Sparse reduced-rank regression for simultaneous dimension reduction and variable selection. *Journal of the American Statistical Association*, 107(500):1533–1545.

- Chen, Y., Goldsmith, J., and Ogden, R. T. (2016). Variable selection in function-on-scalar regression. *Stat*, 5(1):88–101.
- Crainiceanu, C., Ruppert, D., and Wand, M. P. (2005). Bayesian analysis for penalized spline regression using WinBUGS. *Journal of Statistical Software*, 14(14):1–24.
- Crainiceanu, C. M. and Goldsmith, A. J. (2010). Bayesian functional data analysis using WinBUGS. *Journal of Statistical Software*, 32(11).
- Dean, D. A., Goldberger, A. L., Mueller, R., Kim, M., Rueschman, M., Mobley, D., Sahoo, S. S., Jayapandian, C. P., Cui, L., Morrical, M. G., et al. (2016). Scaling up scientific discovery in sleep medicine: the National Sleep Research Resource. *Sleep*, 39(5):1151–1164.
- Fan, Z. and Reimherr, M. (2017). High-dimensional adaptive function-on-scalar regression. *Econometrics and Statistics*, 1:167–183.
- Gelman, A. (2006). Prior distributions for variance parameters in hierarchical models (comment on article by Browne and Draper). *Bayesian Analysis*, 1(3):515–534.
- George, E. I. and McCulloch, R. E. (1997). Approaches for Bayesian variable selection. *Statistica Sinica*, pages 339–373.
- Gilks, W. R., Richardson, S., and Spiegelhalter, D. (1995). *Markov chain Monte Carlo in practice*. CRC press.
- Goldsmith, J., Greven, S., and Crainiceanu, C. (2013). Corrected confidence bands for functional data using principal components. *Biometrics*, 69(1):41–51.
- Goldsmith, J. and Kitago, T. (2016). Assessing systematic effects of stroke on motor control by using hierarchical function-on-scalar regression. *Journal of the Royal Statistical Society: Series C (Applied Statistics)*, 65(2):215–236.

- Goldsmith, J., Scheipl, F., Huang, L., Wrobel, J., Gellar, J., Harezlak, J., McLean, M. W., Swihart, B., Xiao, L., Crainiceanu, C., and Reiss, P. T. (2016). *refund: Regression with Functional Data*. R package version 0.1-16.
- Goldsmith, J., Zipunnikov, V., and Schrack, J. (2015). Generalized multilevel function-on-scalar regression and principal component analysis. *Biometrics*, 71(2):344–353.
- Guo, W. (2002). Functional mixed effects models. *Biometrics*, 58(1):121–128.
- Hahn, P. R. and Carvalho, C. M. (2015). Decoupling shrinkage and selection in Bayesian linear models: a posterior summary perspective. *Journal of the American Statistical Association*, 110(509):435–448.
- Ishwaran, H. and Rao, J. S. (2005). Spike and slab variable selection: frequentist and Bayesian strategies. *The Annals of Statistics*, 33(2):730–773.
- Kowal, D. R. (2018). Dynamic function-on-scalars regression. *arXiv preprint arXiv:1806.01460*.
- Kowal, D. R., Matteson, D. S., and Ruppert, D. (2017a). A Bayesian multivariate functional dynamic linear model. *Journal of the American Statistical Association*, 112(518):733–744.
- Kowal, D. R., Matteson, D. S., and Ruppert, D. (2017b). Dynamic shrinkage processes. *arXiv preprint arXiv:1707.00763*.
- Meyer, M. J., Coull, B. A., Versace, F., Cinciripini, P., and Morris, J. S. (2015). Bayesian function-on-function regression for multilevel functional data. *Biometrics*, 71(3):563–574.
- Mitchell, T. J. and Beauchamp, J. J. (1988). Bayesian variable selection in linear regression. *Journal of the American Statistical Association*, 83(404):1023–1032.
- Montagna, S., Tokdar, S. T., Neelon, B., and Dunson, D. B. (2012). Bayesian latent factor regression for functional and longitudinal data. *Biometrics*, 68(4):1064–1073.

- Morris, J. S. (2015). Functional regression. *Annual Review of Statistics and Its Application*, 2:321–359.
- Morris, J. S. and Carroll, R. J. (2006). Wavelet-based functional mixed models. *Journal of the Royal Statistical Society: Series B (Statistical Methodology)*, 68(2):179–199.
- Neal, R. M. (2003). Slice sampling. *Annals of Statistics*, pages 705–741.
- O’Hara, R. B. and Sillanpää, M. J. (2009). A review of Bayesian variable selection methods: what, how and which. *Bayesian Analysis*, 4(1):85–117.
- Piironen, J. and Vehtari, A. (2016). On the hyperprior choice for the global shrinkage parameter in the horseshoe prior. *arXiv preprint arXiv:1610.05559*.
- Polson, N. G. and Scott, J. G. (2010). Shrink globally, act locally: sparse Bayesian regularization and prediction. *Bayesian Statistics*, 9:501–538.
- Polson, N. G., Scott, J. G., and Windle, J. (2013). Bayesian inference for logistic models using Pólya–Gamma latent variables. *Journal of the American Statistical Association*, 108(504):1339–1349.
- Ramsay, J. and Silverman, B. (2005). *Functional Data Analysis*. Springer.
- Reiss, P. T., Huang, L., and Mennes, M. (2010). Fast function-on-scalar regression with penalized basis expansions. *The International Journal of Biostatistics*, 6(1).
- Rue, H. (2001). Fast sampling of Gaussian Markov random fields. *Journal of the Royal Statistical Society: Series B (Statistical Methodology)*, 63(2):325–338.
- Ruppert, D. (2002). Selecting the number of knots for penalized splines. *Journal of Computational and Graphical Statistics*, 11(4).
- Ruppert, D., Wand, M. P., and Carroll, R. J. (2003). *Semiparametric regression*. Number 12. Cambridge University Press.

- Shang, H. L. (2014). A survey of functional principal component analysis. *Advances in Statistical Analysis*, 98(2):121–142.
- Suarez, A. J., Ghosal, S., et al. (2017). Bayesian estimation of principal components for functional data. *Bayesian Analysis*, 12(2):311–333.
- Wand, M. P., Ormerod, J. T., Padoan, S. A., and Frühwirth, R. (2011). Mean field variational Bayes for elaborate distributions. *Bayesian Analysis*, 6(4):847–900.
- Wang, L., Chen, G., and Li, H. (2007). Group SCAD regression analysis for microarray time course gene expression data. *Bioinformatics*, 23(12):1486–1494.
- Wood, S. (2006). *Generalized additive models: an introduction with R*. CRC press.
- Xiao, L., Li, Y., and Ruppert, D. (2013). Fast bivariate p-splines: the sandwich smoother. *Journal of the Royal Statistical Society: Series B (Statistical Methodology)*, 75(3):577–599.
- Yang, Y. and Zou, H. (2017). *gglasso: Group Lasso Penalized Learning Using a Unified BMD Algorithm*. R package version 1.4.
- Yuan, M. and Lin, Y. (2006). Model selection and estimation in regression with grouped variables. *Journal of the Royal Statistical Society: Series B (Statistical Methodology)*, 68(1):49–67.
- Zhang, G.-Q., Cui, L., Mueller, R., Tao, S., Kim, M., Rueschman, M., Mariani, S., Mobley, D., and Redline, S. (2018). The National Sleep Research Resource: towards a sleep data commons. *Journal of the American Medical Informatics Association*.
- Zhu, H., Brown, P. J., and Morris, J. S. (2011). Robust, adaptive functional regression in functional mixed model framework. *Journal of the American Statistical Association*, 106(495):1167–1179.

Appendix

MCMC Sampling Algorithm

1. **Imputation:** $[Y_i(\tau_i^*) | \dots] \stackrel{indep}{\sim} N(\sum_k f_k(\tau_i^*)\beta_{k,i}, \sigma_\epsilon^2)$ for all unobserved $Y_i(\tau_i^*)$.
2. **Loading curves and smoothing parameters:** for $k = 1, \dots, K$,
 - (a) $[\lambda_{f_k} | \dots] \sim \text{Gamma}((L_m - D + 1 + 1)/2, \boldsymbol{\psi}'_k \boldsymbol{\Omega} \boldsymbol{\psi}_k / 2)$ truncated to $(10^{-8}, \infty)$.
 - (b) $[\boldsymbol{\psi}_k | \dots] \sim N(\mathbf{Q}_{\boldsymbol{\psi}_k}^{-1} \boldsymbol{\ell}_{\boldsymbol{\psi}_k}, \mathbf{Q}_{\boldsymbol{\psi}_k}^{-1})$ conditional on $\mathbf{C}_k \boldsymbol{\psi}_k = \mathbf{0}$, where $\mathbf{Q}_{\boldsymbol{\psi}_k} = \sigma_\epsilon^{-2} (\mathbf{B}' \mathbf{B}) \sum_{i=1}^n \beta_{k,i}^2 + \lambda_{f_k} \boldsymbol{\Omega}$, $\boldsymbol{\ell}_{\boldsymbol{\psi}_k} = \sigma_\epsilon^{-2} \mathbf{B}' \sum_{i=1}^n [\beta_{k,i} (\mathbf{Y}_i - \sum_{k' \neq k} \mathbf{f}_{k'} \beta_{k',i})]$, $\mathbf{C}_k = (\mathbf{f}_1, \dots, \mathbf{f}_{k-1}, \mathbf{f}_{k+1}, \dots, \mathbf{f}_K)' \mathbf{B} = (\boldsymbol{\psi}_1, \dots, \boldsymbol{\psi}_{k-1}, \boldsymbol{\psi}_{k+1}, \dots, \boldsymbol{\psi}_K)'$ using the following:
 - i. $\boldsymbol{\psi}_k^0 \sim N(\mathbf{Q}_{\boldsymbol{\psi}_k}^{-1} \boldsymbol{\ell}_{\boldsymbol{\psi}_k}, \mathbf{Q}_{\boldsymbol{\psi}_k}^{-1})$ using Algorithm 1;
 - ii. Use forward substitution to obtain $\bar{\mathbf{C}}$ as the solution to $\bar{\mathbf{Q}}_L \bar{\mathbf{C}} = \mathbf{C}_k$, then use backward substitution to obtain $\tilde{\mathbf{C}}$ as the solution to $\bar{\mathbf{Q}}_L' \tilde{\mathbf{C}} = \bar{\mathbf{C}}$;
 - iii. Set $\boldsymbol{\psi}_k^* = \boldsymbol{\psi}_k^0 - \tilde{\mathbf{C}} (\mathbf{C}_k \tilde{\mathbf{C}})^{-1} \mathbf{C}_k \boldsymbol{\psi}_k^0$;
 - iv. Retain the vectors $\boldsymbol{\psi}_k = \boldsymbol{\psi}_k^* / \sqrt{\boldsymbol{\psi}_k^{*'} \mathbf{B}' \mathbf{B} \boldsymbol{\psi}_k^*} = \boldsymbol{\psi}_k^* / \|\boldsymbol{\psi}_k^*\|$ and $\mathbf{f}_k = \mathbf{B} \boldsymbol{\psi}_k$ and update $\beta_{k,i} \leftarrow \beta_{k,i} \|\boldsymbol{\psi}_k^*\|$.
3. **Project:** update $y_{k,i} = \mathbf{f}'_k \mathbf{Y}_i = \boldsymbol{\psi}'_k (\mathbf{B}' \mathbf{Y}_i)$ for all k, i .
4. **Regression coefficients and subject-specific effects:**
 - (a) $[\boldsymbol{\alpha}_k | \mathbf{Y}, \dots] \sim N(\mathbf{Q}_{\boldsymbol{\alpha}_k}^{-1} \boldsymbol{\ell}_{\boldsymbol{\alpha}_k}, \mathbf{Q}_{\boldsymbol{\alpha}_k}^{-1})$ for $k = 1, \dots, K$ using Algorithm 1 if $p < n$ or Algorithm 2 if $p > n$, where $\mathbf{Q}_{\boldsymbol{\alpha}_k} = \mathbf{X}' \boldsymbol{\Sigma}_{y_k}^{-1} \mathbf{X} + \boldsymbol{\Sigma}_{\boldsymbol{\alpha}_k}^{-1}$ and $\boldsymbol{\ell}_{\boldsymbol{\alpha}_k} = \mathbf{X}' \boldsymbol{\Sigma}_{y_k}^{-1} \mathbf{y}_k$ for $n \times (p+1)$ design matrix \mathbf{X} , marginal variance $\boldsymbol{\Sigma}_{y_k} = \text{diag}(\{\sigma_{\gamma_{k,i}}^2 + \sigma_\epsilon^2\}_{i=1}^n)$, prior variance $\boldsymbol{\Sigma}_{\boldsymbol{\alpha}_k} = \text{diag}(\sigma_{\mu_k}^2, \sigma_{\alpha_{1,k}}^2, \dots, \sigma_{\alpha_{p,k}}^2)$, and projected data $\mathbf{y}_k = (y_{k,1}, \dots, y_{k,n})'$.
 - (b) $[\gamma_{k,i} | \mathbf{Y}, \{\mu_k, \alpha_{j,k}\}, \dots] \stackrel{indep}{\sim} N(Q_{\gamma_{k,i}}^{-1} \ell_{\gamma_{k,i}}, Q_{\gamma_{k,i}}^{-1})$ for $i = 1, \dots, n$ and $k = 1, \dots, K$, where $Q_{\gamma_{k,i}} = \sigma_\epsilon^{-2} + \sigma_{\gamma_{k,i}}^{-2}$ and $\ell_{\gamma_{k,i}} = \sigma_\epsilon^{-2} (y_{k,i} - \mu_k - \sum_{j=1}^p x_{i,j} \alpha_{j,k})$.
5. **Variance parameters:**

(a) **Observation error variance:** $[\sigma_\epsilon^{-2} | \dots] \sim \text{Gamma}\left(\frac{mn}{2}, \frac{1}{2} \sum_{i=1}^n \|\mathbf{Y}_i - \mathbf{F}\boldsymbol{\beta}_i\|^2\right)$

(b) **Multiplicative Gamma Process Parameters:** given μ_k and $\gamma_{k,i}$,

i. $[\delta_{\mu_1} | \dots] \sim \text{Gamma}\left(a_{\mu_1} + \frac{K}{2}, 1 + \frac{1}{2} \sum_{k=1}^K \tau_{\mu_k}^{(1)} \mu_k^2\right)$ and $[\delta_{\mu_\ell} | \dots] \sim \text{Gamma}\left(a_{\mu_2} + \frac{K-\ell+1}{2}, 1 + \frac{1}{2} \sum_{k=\ell}^K \tau_{\mu_k}^{(\ell)} \mu_k^2\right)$ for $\ell > 1$ and $\tau_{\mu_\ell}^{(k)} = \prod_{h=1, h \neq k}^{\ell} \delta_{\mu_h}$.

ii. Set $\sigma_{\mu_k} = \prod_{\ell \leq k} \delta_{\mu_\ell}^{-1/2}$.

iii. $[\delta_{\gamma_1} | \dots] \sim \text{Gamma}\left(a_{\gamma_1} + \frac{Kn}{2}, 1 + \frac{1}{2} \sum_{k=1}^K \tau_{\gamma_k}^{(1)} \sum_{i=1}^n \gamma_{k,i}^2 \xi_{\gamma_{k,i}}\right)$ and $[\delta_{\gamma_\ell} | \dots] \sim \text{Gamma}\left(a_{\gamma_2} + \frac{(K-\ell+1)n}{2}, 1 + \frac{1}{2} \sum_{k=\ell}^K \tau_{\gamma_k}^{(\ell)} \sum_{i=1}^n \gamma_{k,i}^2 \xi_{\gamma_{k,i}}\right)$ for $\ell > 1$ and $\tau_{\gamma_\ell}^{(k)} = \prod_{h=1, h \neq k}^{\ell} \delta_{\gamma_h}$.

iv. Set $\sigma_{\gamma_k} = \prod_{\ell \leq k} \delta_{\gamma_\ell}^{-1/2}$

v. $[\xi_{\gamma_{k,i}} | \dots] \stackrel{\text{indep}}{\sim} \text{Gamma}\left(\frac{\nu_\gamma}{2} + \frac{1}{2}, \frac{\nu_\gamma}{2} + \frac{\gamma_{k,i}^2}{2\sigma_{\gamma_k}^2}\right)$

vi. Set $\sigma_{\gamma_{k,i}} = \sigma_{\gamma_k} / \sqrt{\xi_{\gamma_{k,i}}}$.

(c) **Hierarchical Half-Cauchy Parameters:** using parameter expansions for the half-Cauchy distribution (Wand et al., 2011),

i. $[\sigma_{\alpha_{j,k}}^{-2} | \dots] \stackrel{\text{indep}}{\sim} \text{Gamma}\left(1, \xi_{\alpha_{j,k}} + \alpha_{j,k}^2/2\right)$, $[\xi_{\alpha_{j,k}} | \dots] \stackrel{\text{indep}}{\sim} \text{Gamma}\left(1, \lambda_j^{-2} + \alpha_{j,k}^{-2}\right)$.

ii. $[\lambda_j^{-2} | \dots] \stackrel{\text{indep}}{\sim} \text{Gamma}\left(\frac{K+1}{2}, \xi_{\lambda_j} + \sum_{k=1}^K \xi_{\lambda_{j,k}}\right)$, $[\xi_{\lambda_j} | \dots] \stackrel{\text{indep}}{\sim} \text{Gamma}\left(1, \lambda_0^{-2} + \lambda_j^{-2}\right)$.

iii. $[\lambda_0^{-2} | \dots] \sim \text{Gamma}\left(\frac{p+1}{2}, \xi_{\lambda_0} + \sum_{j=1}^p \xi_{\lambda_j}\right)$, $[\xi_{\lambda_0} | \dots] \sim \text{Gamma}\left(1, p + \lambda_0^{-2}\right)$.

6. **Hyperparameters:** sample $a_{\mu_1}, a_{\mu_2}, a_{\gamma_1}, a_{\gamma_2}$, and ν_γ independently using the slice sampler (Neal, 2003).

The sampling algorithms for the regression coefficients are as follows:

Algorithm 1. ($p < n$)

1. Sample $\boldsymbol{\delta} \sim N(\mathbf{0}, \mathbf{I}_n)$.
2. Compute the (lower triangular) Cholesky decomposition $\mathbf{Q}_{\alpha_k} = \bar{\mathbf{Q}}_L \bar{\mathbf{Q}}_L'$.
3. Use forward substitution to obtain $\bar{\boldsymbol{\ell}}$ as the solution to $\bar{\mathbf{Q}}_L \bar{\boldsymbol{\ell}} = \boldsymbol{\ell}_{\alpha_k}$.
4. Use backward substitution to obtain $\boldsymbol{\alpha}_k^*$ as the solution to $\bar{\mathbf{Q}}_L' \boldsymbol{\alpha}_k^* = \bar{\boldsymbol{\ell}} + \boldsymbol{\delta}$.

Algorithm 2. ($p > n$)

1. Sample $\mathbf{u} \sim N(\mathbf{0}, \Sigma_{\alpha_k})$ and $\boldsymbol{\delta} \sim N(\mathbf{0}, \mathbf{I}_n)$ independently.
2. Compute $\mathbf{X}_k = \Sigma_{y_k}^{-1/2} \mathbf{X}$ for $\Sigma_{y_k}^{-1/2} = \text{diag}(1/\sqrt{\sigma_{\gamma_{k,i}}^2 + \sigma_\epsilon^2})$.
3. Set $\mathbf{v} = \mathbf{X}_k \mathbf{u} + \boldsymbol{\delta}$.
4. Solve $(\mathbf{X}_k \Sigma_{\alpha_k} \mathbf{X}_k' + \mathbf{I}_n) \mathbf{w} = (\Sigma_{y_k}^{-1/2} \mathbf{y}_k - \mathbf{v})$ to obtain \mathbf{w} .
5. Set $\boldsymbol{\alpha}_k^* = \mathbf{u} + \Sigma_{\alpha_k} \mathbf{X}_k' \mathbf{w}$.

Additional Results

Proof (Theorem 1). We compute $\mathbb{E}_{[\tilde{\mathbf{Y}}|\mathbf{Y}]} \|h(\tilde{\mathbf{Y}}) - g(\tilde{\boldsymbol{\Delta}}; \tilde{\mathbf{x}})\|_2^2 = \mathbb{E}_{[\boldsymbol{\theta}|\mathbf{Y}]} \left[\mathbb{E}_{[\tilde{\mathbf{Y}}|\boldsymbol{\theta}]} \|h(\tilde{\mathbf{Y}}) - g(\tilde{\boldsymbol{\Delta}}; \tilde{\mathbf{x}})\|_2^2 \right]$ in two steps: (i) $\mathbb{E}_{[\tilde{\mathbf{Y}}|\boldsymbol{\theta}]} \|h(\tilde{\mathbf{Y}}) - g(\tilde{\boldsymbol{\Delta}}; \tilde{\mathbf{x}})\|_2^2 = \mathbb{E}_{[\tilde{\mathbf{Y}}|\boldsymbol{\theta}]} \left\| \left[h(\tilde{\mathbf{Y}}) - \hat{h}_\theta \right] - \left[\hat{h}_\theta - g(\tilde{\boldsymbol{\Delta}}; \tilde{\mathbf{x}}) \right] \right\|_2^2 = \hat{v}_\theta + \|\hat{h}_\theta - g(\tilde{\boldsymbol{\Delta}}; \tilde{\mathbf{x}})\|_2^2$, where $\hat{v}_\theta \equiv \mathbb{E}_{[\tilde{\mathbf{Y}}|\boldsymbol{\theta}]} \|h(\tilde{\mathbf{Y}}) - \hat{h}_\theta\|_2^2 < \infty$ and $\hat{h}_\theta \equiv \mathbb{E}_{[\tilde{\mathbf{Y}}|\boldsymbol{\theta}]} h(\tilde{\mathbf{Y}})$ may depend on $\boldsymbol{\theta}$, and (ii) $\mathbb{E}_{[\boldsymbol{\theta}|\mathbf{Y}]} \left[\hat{v}_\theta + \|\hat{h}_\theta - g(\tilde{\boldsymbol{\Delta}}; \tilde{\mathbf{x}})\|_2^2 \right] = \bar{v} + \mathbb{E}_{[\boldsymbol{\theta}|\mathbf{Y}]} \left\| \left[\hat{h}_\theta - \bar{h} \right] + \left[\bar{h} - g(\tilde{\boldsymbol{\Delta}}; \tilde{\mathbf{x}}) \right] \right\|_2^2 = \bar{v} + \mathbb{E}_{[\boldsymbol{\theta}|\mathbf{Y}]} \|\hat{h}_\theta - \bar{h}\|_2^2 + \|\bar{h} - g(\tilde{\boldsymbol{\Delta}}; \tilde{\mathbf{x}})\|_2^2$, where $\bar{v} = \mathbb{E}_{[\boldsymbol{\theta}|\mathbf{Y}]}(\hat{v}_\theta)$ and $\bar{h} = \mathbb{E}_{[\boldsymbol{\theta}|\mathbf{Y}]}(\hat{h}_\theta)$. Since only the last term depends on $\tilde{\boldsymbol{\Delta}}$, this proves the result. \square

Proof (Theorem 2). Let $\mathcal{L}(\tilde{\mathbf{Y}}_i, \boldsymbol{\Delta}|\mathbf{F}) = \|\tilde{\mathbf{Y}}_i - \mathbf{F}\boldsymbol{\delta}_0 - \mathbf{F}\boldsymbol{\Delta}\tilde{\mathbf{x}}_i\|_2^2$ and let $\boldsymbol{\theta}_{-\mathbf{F}}$ denote model parameters excluding \mathbf{F} . Denoting all conditional densities $p(\cdot|\cdot)$,

$$\begin{aligned} \mathbb{E}_{[\mathbf{F}|\mathbf{Y}]} \left\{ \mathbb{E}_{[\tilde{\mathbf{Y}}|\mathbf{F}, \mathbf{Y}]} \mathcal{L}(\tilde{\mathbf{Y}}, \boldsymbol{\Delta}|\mathbf{F}) \right\} &= \int p(\mathbf{F}|\mathbf{Y}) \left\{ \int p(\tilde{\mathbf{Y}}|\mathbf{F}, \mathbf{Y}) \mathcal{L}(\tilde{\mathbf{Y}}, \boldsymbol{\Delta}|\mathbf{F}) d\tilde{\mathbf{Y}} \right\} d\mathbf{F} \\ &= \int p(\mathbf{F}|\mathbf{Y}) \left\{ \int \left[\int p(\tilde{\mathbf{Y}}|\boldsymbol{\theta}) p(\boldsymbol{\theta}_{-\mathbf{F}}|\mathbf{F}, \mathbf{Y}) d\boldsymbol{\theta}_{-\mathbf{F}} \right] \mathcal{L}(\tilde{\mathbf{Y}}, \boldsymbol{\Delta}|\mathbf{F}) d\tilde{\mathbf{Y}} \right\} d\mathbf{F} \\ &= \int p(\boldsymbol{\theta}|\mathbf{Y}) \left\{ \int p(\tilde{\mathbf{Y}}|\boldsymbol{\theta}) \mathcal{L}(\tilde{\mathbf{Y}}, \boldsymbol{\Delta}|\mathbf{F}) d\tilde{\mathbf{Y}} \right\} d\boldsymbol{\theta} \\ &= \mathbb{E}_{[\boldsymbol{\theta}|\mathbf{Y}]} \left\{ \mathbb{E}_{[\tilde{\mathbf{Y}}|\boldsymbol{\theta}]} \mathcal{L}(\tilde{\mathbf{Y}}, \boldsymbol{\Delta}|\mathbf{F}) \right\} \end{aligned}$$

The remainder of the proof follows Theorem 1 using $h(y) = y$ and $g(\tilde{\boldsymbol{\Delta}}, \tilde{\mathbf{x}}) = \tilde{\boldsymbol{\Delta}}\tilde{\mathbf{x}} = \mathbf{F}\boldsymbol{\Delta}\tilde{\mathbf{x}}$, subject to one modification. Ignoring the intercept for simplicity, $\hat{h}_\theta = \mathbb{E}_{[\tilde{\mathbf{Y}}|\boldsymbol{\theta}]} h(\tilde{\mathbf{Y}}) = \tilde{\mathbf{A}}\tilde{\mathbf{x}} = \mathbf{F}\mathbf{A}\tilde{\mathbf{x}}$, which implies $\|\hat{h}_\theta - g(\tilde{\boldsymbol{\Delta}}; \tilde{\mathbf{x}})\|_2^2 = \|\mathbf{F}\mathbf{A}\tilde{\mathbf{x}} - \mathbf{F}\boldsymbol{\Delta}\tilde{\mathbf{x}}\|_2^2 = \|\mathbf{A}\tilde{\mathbf{x}} - \boldsymbol{\Delta}\tilde{\mathbf{x}}\|_2^2$ using the orthonormality of \mathbf{F} . The result follows immediately. \square

Item name	Factors	Question
bcksleep	missing/low/high	Past 4 Weeks: Trouble Getting Back To Sleep After You Waking Too Early
bedtmwkd	missing/5-7/8-9/10-11/later	Bedtime Weekday
car	missing/low/high	Chance Of Dozing / Fall Asleep While: In Car Stopped In Traffic
dinner	low/high	Chance Of Dozing / Fall Asleep While: At Dinner Table
driving	low/high	Chance Of Dozing / Fall Asleep While: While Driving
extrahrs	missing/low/high	Days Per Month Working Extra Hours Beyond Usual Schedule
feelngbstpk	missing/low/high	Time Of Day Reaching Best Feeling Peak
feelngbstr	high/low	Time Of Day Feeling Best
insmnia	missing/no/yes	Told By Doctor As Having: Insomnia
irritable	low/high	Past 4 Weeks: Have Sleep Difficulties Causing Irritability
legsdscmfrt	missing/no/yes	Experience Desire To Move Legs Because Of Discomfort / Disagreeable Sensations In Legs
lyngdwn	high/low	Chance Of Dozing / Fall Asleep While: Lying Down To Rest In Afternoon
mosttired	missing/low/high	Time In Evening Feel Most Tired And In Need Of Sleep
nap	missing/low/high	Usual Week: Number Of Naps (5 Minutes Or More)
quietly	missing/low/high	Chance Of Dozing / Fall Asleep While: Sitting Quietly After Lunch (No Alcohol)
readng	missing/low/high	Chance Of Dozing / Fall Asleep While: Sitting And Reading
riding	missing/low/high	Chance Of Dozing / Fall Asleep While: Riding As Passenger In Car
rstlesslgs	missing/no/yes	Told By Doctor As Having: Restless Legs
rubbnglgs	missing/no/yes	Feel Need To Move To Relieve Discomfort By Walking Or Rub Legs
sittng	missing/low/high	Chance Of Dozing / Fall Asleep While: Sitting Inactive In Public
sleepy	missing/low/high	Past 4 Weeks: Feel Overly Sleepy During Day
slpapnea	no/yes	Told By Doctor As Having: Sleep Apnea
slpngpills	missing/low/high	Past 4 Weeks: Take Sleeping Pills To Help Sleep
snored	missing/low/high	Past 4 Weeks: Snored
stpbrthng	missing/low/high	Past 4 Weeks: Stop Breathing During Sleep
talkng	low/high	Chance Of Dozing / Fall Asleep While: Sitting And Talking To Someone
tired	missing/low/high	How Tired During First Half Hour After Having Woken In Morning
trbleslpng	low/high	Past 4 Weeks: Trouble Falling Asleep
tv	missing/low/high	Chance Of Dozing / Fall Asleep While: Watching TV
types	missing/evening/morning/neither	Type Of Person: Morning Or Evening
typicalslp	missing/low/high	Past 4 Weeks: Overall Typical Night Sleep
wakeearly	missing/no/yes	Wake up earlier than planned
wakeup	yes/no	Wake up several times a night
wkdaysleepdur	missing/<7/7-9/>9	Sleep duration weekday (hours)

Table 2: Questionnaire items included in the model and corresponding variable levels. The first level in each row is the contrasting variable.